Published in final edited form as:
Physiol Genomics. 2005 October 17; 23(2): 192–205. doi:10.1152/physiolgenomics.00112.2005.

Microarray analysis reveals novel gene expression changes associated with erectile dysfunction in diabetic rats

Chris J. Sullivan[1], **Thomas H. Teal**[1], **Ian P. Luttrell**[1], **Khoa B. Tran**[1], **Mette A. Peters**[2,*], and **Hunter Wessells**[1]

[1]Department of Urology, University of Washington, School of Medicine and Harborview Medical Center, Seattle, WA 98104

[2]Center for Expression Arrays, University of Washington, Seattle, WA 98195

Abstract

To investigate the full range of molecular changes associated with erectile dysfunction (ED) in type 1 diabetes, we examined alterations in penile gene expression in streptozotocin-induced diabetic rats and littermate controls. Using Affymetrix GeneChip arrays and statistical filtering, 529 genes/transcripts were considered to be differentially expressed in the diabetic rat cavernosum as compared to control. Gene Ontology (GO) classification indicated that there was a decrease in numerous extracellular matrix genes (e.g., collagen and elastin related) and an increase in oxidative-stress genes in the diabetic rat cavernosum. In addition, PubMatrix literature mining identified differentially expressed genes previously shown to mediate vascular dysfunction (e.g., Cp, Lpl, Cd36) as well as genes involved in modulation of smooth muscle phenotype (e.g., Klf5, Cx3cl1). Real-time PCR was used to confirm changes in expression for 23 relevant genes. Further validation of ceruloplasmin (Cp) expression in the diabetic rat cavernosum demonstrated increased mRNA levels of the secreted and anchored splice variants of Cp. CP protein levels showed a 1.9-fold increase in tissues from diabetic rats versus controls. Immunohistochemistry demonstrated localization of CP protein in the cavernosal sinusoids of control and diabetic animals, including the endothelial and smooth muscle layers. Overall, this study broadens the scope of candidate genes and pathways that may be relevant to the pathophysiology of diabetes-induced ED as well as highlights the potential complexity of this disorder.

Keywords

cavernosum; penis; erectile dysfunction; gene ontology; diabetic

Introduction

Erectile dysfunction (ED) has origins associated with a complex interplay of factors ranging from psychosocial disorders (e.g., depression) to nerve injury (e.g., prostatectomy) to vascular pathologies (e.g., hypertension, atherosclerosis). Of all co-morbid medical conditions, diabetes mellitus imparts the greatest risk of ED. Men with diabetes have a greater prevalence of ED and earlier onset of the condition as compared to the general population (34, 101). Furthermore, men with diabetes present with more severe dysfunction and are less responsive to current pharmacological therapies for ED (14, 47, 91).

All correspondence should be addressed to: Hunter Wessells, M.D., F.A.C.S., Department of Urology, Harborview Medical Center, 325 9th Avenue, Box 359868, Seattle, WA 98104-2499, Tel (206) 731-3205, Fax (206) 341-5442, wessells@u.washington.edu.
*Rosetta Biosoftware, Seattle, WA 98109 (Current Address)

Penile erection is a complex and integrated neurovascular event (4). Since diabetes leads to neural and vascular pathologies, it has the potential to impact all components of the erectile response. Structurally, the erectile apparatus consists of paired organs (corpora cavernosa) that run the length of the penis. Each cavernosum is a specialized vascular compartment with sinusoidal trabeculae supporting a thick smooth muscle layer lined by endothelial cells. The arterial supply of the penis gives rise to helicine resistance arteries which open directly into the sinusoidal spaces of the cavernosa (108). During erection, nitric oxide (NO) produced by nitrergic nerves (autonomic neurons containing neuronal NO synthase; nNOS) and endothelial cells (endothelial NO synthase; eNOS) stimulates relaxation of smooth muscle in the penile circulation and corpora cavernosa (108). In the smooth muscle cells, NO binds soluble guanylate cyclase thus increasing cGMP levels and stimulating cGMP-dependent protein kinase I (Prkg1 alias cGKI) which ultimately leads to relaxation (49). The ensuing arterial inflow and expansion of the cavernosa against the tunica albuginea (dense connective tissue surrounding the cavernosa) leads to compression of subtunical veins that impede blood outflow, producing a rigid erection.

Although recent studies have been instrumental in establishing mechanisms of impaired diabetic erectile function (see recent reviews [7, 11]), it is likely that the molecules and pathways identified to date represent only a small portion of the total changes occurring in erectile tissues that are due to diabetes. Thus, the current study was designed to take a global approach to investigate the range of molecular changes in cavernosal tissue from animals with diabetes-associated ED. The ultimate goal is to advance our understanding of the pathogenesis of diabetes-associated ED and to help provide a rationale for novel treatments and preventive therapies.

Methods

Animals and induction of diabetes

Male Fischer 344 rats (Taconic Farms) were housed in groups of 2–3 in a specific pathogen-free environment. Rats were maintained in a temperature-controlled room with 12:12h light dark cycle and received food and water *ad libitum*. All procedures were approved by the Animal Care and Use Committee at the University of Washington and were performed in accordance with NIH Guidelines for the Care and Use of Animals. At 2 months of age, rats were separated into individual cages and injected intraperitoneally with 35 mg streptozotocin (STZ; Sigma Chemical) per kg body weight in sterile citrate buffer to induce diabetes. Control rats were injected with an equivalent volume of citrate buffer. Twenty-four hr after injections, blood glucose was checked via tail stick using an Accu-Check glucose monitor (Roche Diagnostics). Animals were considered diabetic if their blood glucose levels were above 300 mg/dL. Body weight and glucose levels were monitored weekly in all animals over the course of the study (10 weeks). Ten-weeks duration of diabetes was selected based on previous studies demonstrated significantly reduced erectile responses in Fischer 344 rats following 8–12 weeks of diabetes (26, 98). Values are presented as the mean ± SE. Comparison between two means was performed using Student's unpaired *t*-test.

Measurement of erectile responses

Ten weeks after induction of diabetes, intracavernosal pressure (ICP) changes in response to cavernous nerve stimulation were measured in control (n=8) and diabetic rats (n=6) as described previously (125). Briefly, anesthesia was induced with 5% isoflurane (Novaplus) vaporized in 100% O_2 and then maintained with 1.5% isoflurane during the procedures. The right carotid artery was cannulated to monitor arterial blood pressure. The penis was exposed and the corpus spongiosum was mobilized to facilitate insertion of a 25-gauge needle into the corpus cavernosum. The needle was attached via PE-50 tubing to a pressure

transducer (Kent Scientific) filled with heparinized saline. To establish baseline parameters, the cavernous nerve was stimulated (6 V, 10 Hz, 1 min) with a bipolar electrode, Grass S48K nerve stimulator, and stimulus isolation unit SIU5 (Grass Telefactor). Pressure changes were recorded continuously in response to 1, 2, 4, 6, and 10 V stimulations, each for a duration of 1 min with 5 min between voltages. Intracavernous and arterial pressure were converted to analog signals and transmitted to a data acquisition program (Hem 3.2, Notocord). The erectile response was calculated using area under the curve in mmHg for intracavernosal pressure during the 1 min stimulation period (ΔICP). This value was divided by the area under the curve for the calculated mean arterial pressure (MAP) during the same 1 min stimulation (ΔICP/MAP). Groups were compared by one-way ANOVA with a Student-Newman-Keuls multiple comparison test.

Tissue Collection

Immediately following ICP measurements, the penis was rapidly dissected free at the level of the crura. After removal of any overlying skeletal muscle, equal portions of the crura and shaft were placed into1.5 ml tubes, flash frozen in liquid nitrogen, and then stored at −80°C. For histology, a small cross-section of the proximal shaft was suspended in OCT compound (Tissue-Tek), frozen over liquid nitrogen, and stored at −80°C. An independent cohort of control and diabetic F344 rats (n=5 each) was generated and used to collect penile protein samples for Western blotting. The samples were collected as described above and stored at −80°C.

RNA isolation

Total RNA isolation was performed using a combination of Trizol Reagent (Invitrogen) and RNeasy columns (Qiagen). Penile tissue stored at −80°C was gradually thawed using RNAlater-ICE (Ambion) as described by the manufacturer. Next, tissue was homogenized in Trizol Reagent according to the manufacturer's instructions with the following modifications. After addition of chloroform, the centrifugation was performed using Phase Lock Gel Heavy 2 ml tubes (Eppendorf) to improve recovery of the aqueous phase of the solution. One half volume of 100% ethanol was combined with the recovered aqueous solution and the mixture was added to an RNeasy mini column. This and all subsequent steps were performed as described by the manufacturer (Qiagen RNeasy handbook 3rd edition). On-column DNase digestion was done using the Qiagen RNase-Free DNase kit as directed in the RNeasy handbook (appendix D). RNA quality was examined by the RNA 6000 LabChip Kit on the 2100 bioanalyzer (Agilent Technologies). Quantity and absorbance at 260/280 nm of total and cRNA was assessed by UV spectrophotometer. After quantification RNA samples were divided into 5 μg aliquots and stored at −80°C.

Microarray hybridization and data analysis

Double-stranded cDNA was synthesized from total RNA, amplified as cRNA, labeled with biotin, and hybridized to Affymetrix Rat 230A GeneChips, which were washed and scanned at the University of Washington's Center for Expression Arrays according to procedures developed by the manufacturer. A total of 5 control and 5 diabetic samples were used requiring a total of 10 GeneChips. Image processing was done using Affymetrix GCOS software. The quality of hybridization and overall chip performance was determined by visual inspection of the raw scanned data and the GCOS generated report file. The raw data were loaded into the Rosetta Resolver Gene Expression Data Analysis System (Rosetta Biosoftware, Seattle, WA) for analysis utilizing the Rosetta Resolver System error model (97). Based on 5 biological replicates from each experimental condition, Resolver was used to generate 1) *p*-values to determine if genes were detected (i.e., present call), 2) *p*-values from analysis of variance (ANOVA) to establish differentially expressed genes between the

control and diabetic groups, and 3) an estimate of fold change for each gene relative to control. These parameters were used for statistical filtering of the array data as described in the results. The Resolver output values for those genes selected as significant are available in the online supplement. In compliance with MIAME standards, Affymetrix data files (CHP and CEL) have been deposited in the NCBI Gene Expression Omnibus repository (query accession GSE2457). The gene symbols used in this manuscript are, to the best of our knowledge, those designated on NCBI Entrez Gene and every effort was made to avoid the use of ambiguous gene designations. Also, Affymetrix Rat 230A probe set IDs were annotated via the NetAffx™ Analysis Center (www.affymetrix.com) in early 2005. Since the annotations are periodically updated, changes in Affymetrix Probe Set gene designations are possible. GeneChip hybridizations, scanning, and Resolver analysis were performed at the Center for Expression Arrays at the University of Washington.

Real-time PCR

Using the samples from the array experiments (n=5 each group), 2 μg of total RNA was reverse transcribed into cDNA using RETROscript first strand synthesis kit (Ambion). Each cDNA sample was then used as a template for real-time PCR amplification using SYBR Green PCR Master Mix (Applied Biosystems) and forward/reverse primers for the various target genes (see online supplement for primer sequences). Amplification and detection was performed on an Applied Biosystems 7900 Real-Time PCR system according to manufacturer's instructions using a two-stage cycle of 95°C for 15 sec and 62°C for 1 min repeated for 40 cycles followed by a dissociation stage. Threshold cycle (C_T) values were exported into spreadsheets and then relative changes in gene expression were calculated using the $2^{-\Delta\Delta CT}$ method as described previously (73). Results are given as fold change relative to control (non-diabetic) cDNA while using Actb (Beta actin) expression as a reference gene. All samples were prepared and examined in parallel. Conventional, non-quantitative PCR was performed for ceruloplasmin (Cp) to confirm the presence of its two splice variants based on published primer sets (20, 89). A common forward primer was used for both splice variants of Cp, 5'-GTA TGT GAT GGC TAT GGG CAA TGA-3'. The Cp-serum or secreted form was detected using the reverse primer 5'-TCA TCT GTC CAT CGG CAT TA-3', which yields a product size of 374bp. The Cp-GPI or glycosylphosphatidylinositol anchored form was detected using the reverse primer 5'-CCT GGA TGG AAC TGG TGA TGG A-3'and yields a product size of 449bp. cDNA template was amplified using Qiagen Taq PCR core kit on an Eppendorf Mastercycler with the following cycle parameters, 95°C for 15 sec, 57°C for 45 sec, and 72°C for 1 min (repeated for 35 cycles).

Western blotting

Cavernosal tissue was weighed, minced with a razor blade, and homogenized for 30 sec in 10 volumes of ice-cold lysis buffer containing fresh protease inhibitors. Following centrifugation at 16,000g × 20 min at 4°C, supernatant was collected and protein concentrations were determined using the MicroBCA kit (Pierce). Equal amounts of protein (50 μg) were run on pre-cast polyacrylamide gels (GeneMate) and transferred to PVDF membrane (Millipore). The membrane was blocked for 1 hr at room temperature in 5% non-fat milk in 1X PBS containing 0.1% Tween-20. Membranes were incubated for 1 hr at room temperature with primary goat polyclonal anti-human ceruloplasmin antibody (Sigma, C0911, 2 μg/ml) diluted in blocking solution. The primary antibody was detected with HRP-conjugated anti-goat secondary (Amersham Biosciences), diluted 1:1000 in blocking solution and incubated for 1 hr at room temperature. Blots were developed using ECL Chemiluminescent reagents (Amersham Biosciences) and results were quantified by densitometry (LabWorks). Membranes were incubated with mouse monoclonal anti-β-actin antibody (Sigma, AC-15, 1:40,000 dilution) as a reference for protein loading. Values

represent ceruloplasmin densitometry normalized to β-actin and are presented as the mean ± SE. Comparison between means was performed using Student's unpaired *t*-test.

Histology and immunohistochemistry

Frozen penile sections (8 μm) were cut from the OCT embedded tissue blocks and placed on glass slides. For immunohistochemistry, slides were fixed in cold acetone (−20°C) for five minutes, air-dried, and then placed in PBS. As previously described, standard immunohistochemistry techniques were used to identify antigens of interest (126). Incubation with primary antibody was done for 1 hr at 37°C in a humidified chamber. Secondary antibody was applied for 30 min at room temperature. For colocalization staining (e.g., ceruloplasmin and PECAM/CD31), primary and secondary were applied sequentially as described above and then repeated for the next antibody pair. Primary antibodies used and working concentrations: mouse monoclonal anti-rat CD31 (Chemicon, 1393Z, 20 μg/ml), goat polyclonal anti-human ceruloplasmin (Bethyl Laboratories, A80-124A, 5ug/ml). Secondary antibodies used and concentrations: rabbit anti-mouse IgG Alexa 488, donkey anti-goat Alexa 568 (Molecular Probes, 10 μg/ml). Slides were mounted and cover slipped using Gel Mount (Biomeda). Fluorescent images were captured using a Nikon Eclipse E600 microscope integrated with a RT color Spot CCD camera (Diagnostic Instruments). Image processing such as merging of dual labeled sections was done with Spot Advanced software (Diagnostic Instruments).

Results

Glucose levels in diabetic rats

Mean body weight of diabetic rats at week 10 was significantly lower than control (245 ± 8 vs. 377 ± 13 g, respectively, $p < 0.01$). Blood glucose was significantly higher in diabetic rats relative to control (386 ± 8 vs. 94 ± 5 mg/dL, respectively, $p < 0.0001$) and glucose levels in the STZ group were maintained at 300 mg/dL or above throughout the course of the study.

Intracavernosal pressure responses to nerve stimulation demonstrate erectile dysfunction in diabetic rats

At 10 weeks after induction of diabetes, there was decreased erectile function in diabetic animals in response to cavernous nerve stimulation (Figure 1). The mean ΔICP/MAP (area under the curve for the ICP and MAP tracings during the 60 sec stimulation, mmHg·s) was lower at all voltages in the diabetic group compared to control (statistically significant at 4, 6, and 10 volts, $p < 0.01$). This confirmed the presence of diabetes-associated erectile dysfunction in the STZ-treated animals and the observed reductions in ICP/MAP (~30%) are consistent with previously reported values of ICP responses in Fischer-344 diabetic rats which showed approximately 25–40% reductions in ICP depending on the nerve stimulus parameters (98). El-Sakka et al. reported much larger reductions in maximum ICP which were approximately 75% lower in diabetic F-344 rats (26). Examples of the raw ICP and arterial pressure tracings for a representative diabetic and control animal are shown in Figure I of the online supplement. Maximum ICP/MAP was also significantly lower in diabetic rats vs. controls (data not shown).

Array analysis and strategies to determine biological significance

Statistical filtering of the array analysis was based on at least a 1.5 fold change in expression and a Resolver ANOVA $p \leq 0.01$. This *p*-value cutoff was estimated to be equivalent to a false discovery rate of 0.10 (*q*-value) or 10% using the methods of Storey and Tibshirani (110). Genes with detection *p*-values of greater than 0.01 in both groups were considered not

present and were excluded from further analysis. Based on these criteria, 529 genes were considered to be differentially expressed in the diabetic cavernosum (206 upregulated and 323 downregulated). Rosetta Resolver generated values including fold change and *p*-values for the 529 selected genes are available online (supplement) and Affymetrix data files have been submitted to the NCBI Gene Expression Omnibus.

Various strategies were used to examine the 529 changed genes (~350 were annotated genes or homologs) to determine their possible biological relevance to diabetes-associated ED. In particular, the Gene Ontology tool GoMiner was utilized to categorize genes according to biological process, molecular function, and subcellular localization (130). Based on GoMiner analysis, there was significant enrichment of downregulated genes in GO categories such as (# genes down in diabetes per GO catergory / # genes in category on GeneChip): extracellular matrix (ECM) structural constituent (11/39), fibrillar collagen (7/9), ECM structural constituent conferring tensile strength (6/10), skeletal development (13/98), and ossification (5/37). Also, there was an enrichment of upregulated genes in categories such as fatty acid metabolism (12/93), fatty acid oxidation (5/17), and response to oxidative stress (5/44). The entire GoMiner output file (including GO ID, *p*-values, and GO terms) is available in the online supplement. Table 1 shows groupings of genes based on similar Gene Ontology and functional categorization. Many genes are represented by more than one Affymetrix probe set on the RAE230A GeneChip, and in many cases multiple probe sets for the same gene were found to be significant (e.g., Cspg2, Lox, and others as shown in Table 1). The functional grouping of the differentially expressed transcripts shows several elastic fiber-related genes that were downregulated in the diabetic cavernosum (e.g., Cspg2, Lox, Fbn1, and Eln). Similarly, genes encoding a total of 8 different collagen family members were downregulated in the diabetic samples. Various other ECM-related genes were differentially expressed in the diabetic cavernosum, including genes (Spp1, Tnc, and Sparc) that encode members of the functionally grouped matricellular proteins (Table 1).

Using a web-based tool (PubMatrix) for literature mining of PubMed (8), we searched our list of differentially expressed genes against an assortment of terms to identify genes related to vascular biology and/or diabetic complications. The gene lists consisted of official genes names, common names, and gene aliases. Keywords used in the PubMatrix searches included such terms as endothelial dysfunction, vascular function, smooth muscle, aorta, diabetes, and blood vessel. The searches were exported to Microsoft Excel and sorted based on keyword terms to identify possible genes of interest. The ranking of genes with the highest number of PubMed citations for any given keyword was useful to annotate differentially expressed genes in relation to vascular biology and potential processes related to erectile dysfunction. For example, ranking based on the search term “endothelial dysfunction” showed several genes with multiple citations, such as ceruloplasmin (Cp), lipoprotein lipase (Lpl), and Cd36. Alternatively, sorting for citations related to smooth muscle and blood vessels helped to identify numerous differentially expressed genes with potential function in vascular SMC biology, such as Klf5, Cx3cl1, S100a4, C3, Sparc, and Spp1.

Real-time PCR confirmation of array results

We used real-time PCR to examine expression for 23 genes shown to be significantly different by array analysis. These genes were selected based on fold change in expression, GO results, and/or potential role in diabetic complications or vascular biology as identified via PubMatrix. Table 2 shows the fold change estimated by Resolver for the GeneChip data compared to the fold change determined using real-time PCR. The majority of genes showed similar changes in expression when comparing the two methods. One exception is elastase-2 (Ela2) which showed no difference between groups by real-time PCR but had an estimated

4.5-fold change by Resolver analysis. Closer examination of the Resolver data showed very low intensity values for this Affymetrix probe set (1387471_at) in control and diabetic groups. The difficulties of detecting changes in transcripts with very low signal intensity by microarray has been established and this difficulty likely caused Ela2 to be falsely called significant (97). Atp6k was selected as an unchanged gene between diabetic and control groups and this lack of difference was confirmed by the real-time comparison. Overall, the genes examined by real-time PCR showed good agreement with the Resolver estimates of fold change.

Ceruloplasmin gene and protein expression in the rat cavernosum

We decided to examine and validate ceruloplasmin (Cp) expression in cavernosal tissue given that 3 different Affymetrix probe sets all representing the Cp gene were called significant and showed upregulation in the diabetic animals. The Affymetrix NetAffx website was used to identify the specific targets for each Affymetrix probe set. This examination revealed one probe set (1368418_a_at, 3.6-fold increase, $p = 0.0002$) to be aligned with two known Cp splice variants (accessions NM_012532 and AF202115). The other Affymetrix probe sets for Cp have alignment with only one of the splice variants. The Cp-serum or secreted variant (accession NM_012532) is represented by probe set 1368420_at (4.3-fold increase, $p = 0.000006$), whereas probe set 1368419_at (1.9-fold increase, $p = 0.00005$) aligns with only the Cp-glycosylphosphatidylinositol anchored variant (Cp-GPI; accession AF202115). Real-time PCR confirmation of Cp expression was performed and showed a 4.3-fold increase in the diabetic group (Table 2). However, the initial primer set used does not differentiate between Cp splice isoforms because the amplified sequence is shared by both variants. Thus, we took steps to analyze changes in mRNA expression for the individual Cp splice variants in our samples. As shown in Figure 2a, conventional RT-PCR was first used to verify the presence of both Cp isoforms in cavernosal tissue using previously published primers (89). Next, real-time PCR was performed with Cp isoform specific primer sets to differentiate changes in their expression with diabetes. This analysis showed that Cp-GPI had a 2.4-fold increase in the diabetic cavernosum while Cp-serum had an approximately 16-fold increase, although the Cp-GPI variant appeared to be the more abundantly expressed isoform in our samples. A representative amplification plot for each splice isoform in a single diabetic and control animal is shown in Figure 2b. Representative Western blots of CP protein (~130kDa) in diabetic and control cavernosal samples are shown in Figure 2c. Densitometric analysis of CP protein levels, expressed relative to β-actin for each corresponding sample, showed an approximately 1.9-fold increase in diabetic tissue versus control (* $p < 0.05$, Figure 2d).

Immunofluorescence was used to localize CP protein within the cavernosal tissue. Bright CP antibody labeling (red Alexa-568) was observed in the tissue layers lining the cavernosal sinusoids (Figure 3a and 3e). Figure 3d shows the general cavernosal architecture with collagen-based trabeculae lined by smooth muscle cells and a single endothelial cell layer at the blood interface or luminal side. The combined SMC and EC layers are indicated by the black arrowheads in Figure 3d. The brightest CP labeling was often present on the luminal side of the cavernosal sinusoids (Figure 3a) and this staining co-localized with the endothelial marker PECAM/CD31 (Figure 3b; green Alexa-488) as demonstrated by the yellow regions of the merged images in Figure 3c. Thus, it appears that CP is labeling the endothelium and the smooth muscle layers of the cavernosal sinusoids. This is further demonstrated by Figure E showing a higher magnification view of a sinusoid co-stained with CP antibody (red) and CD31/PECAM antibody (green) with the merged image showing CP-CD31 co-labeling in yellow. A similar staining pattern was observed in the penile dorsal vein co-stained with CP and CD31 antibody showing medial SMC and endothelial localization of CP (Figure 3f). Finally, CP antibody labeled small microvessels

adjacent to the cavernosum as shown in Figure 3g. CP staining was observed in punctuate regions of the dorsal nerves adjacent to the cavernosum (data not shown).

Discussion

The present analysis provides a global view of the effect of diabetes on erectile tissue at the mRNA level. This is the first study to use microarrays to examine gene expression in cavernosal tissue from animals with diabetes-associated ED. The identification of approximately 500 differentially expressed genes/transcripts in the diabetic samples underscores the complex nature of this condition and supports the notion that diabetes causes multiple pathophysiological changes in erectile structures of the penis. Determining biological relevance of so many altered genes poses a tremendous challenge. We used several strategies for biological interpretation of our results such as Gene Ontology analysis and mining of the NCBI literature. It is not surprising in diabetes that a large portion of the significantly upregulated genes are involved in pathways required for lipid metabolism. A number of the differentially expressed genes have been previously associated with diabetic complications in other organ systems (see Table 2 for a few examples). This suggests the existence of common molecular pathways underlying the development of diabetic complications in different tissues. Many of the significantly changed genes in our study have no reported role in diabetes and no clear function related to erectile physiology.

Collagen, elastin, and matrix genes

The Gene Ontology analysis highlights the considerable downregulation of extracellular matrix genes in the cavernosal tissue of diabetic rats. The extracellular matrix of human and rat erectile tissues is composed mainly of collagen, elastic fibers, and various proteoglycans (43, 52, 74, 96). Several studies examining human erectile tissues have demonstrated qualitative and quantitative changes in collagen and elastic fibers in the cavernosum of impotent patients (21, 95, 105, 128). Similarly, animal studies show morphological and ultrastructural changes in the cavernosum of diabetic and aged rats (15, 30, 102). To date, the specific pathways and molecules mediating such changes have not been fully elucidated. Mathematical modeling of penile hemodynamics suggests that cavernosal expandability and tunical distensability are important factors contributing to erection (40, 118). Accordingly, diabetes-induced changes in matrix components and ECM structural organization of the tunica albuginea and/or the corpus cavernosum could act to impair erectile function. The current array analysis provides several prospective molecules that could be contributing to alterations in cavernosal structure associated with diabetes.

The concurrent downregulation of genes encoding components of collagens type 1, 3, 5, 6, and 11 (listed in Table 1) certainly suggests that alterations in collagen biosynthesis and/or composition may contribute to the development of ED in this model. We observed decreased diabetic expression of Col1a1 and Col1a2, both of which encode fibrils forming collagen type 1 that provides tissue with tensile strength and stiffness (41). Collagen type 1 is the most abundant form of collagen in human and rat erectile tissues and forms the bulk of the matrix structure of the cavernosum (74, 96). The Col3a1 gene, reduced 2-fold in diabetic cavernosum, encodes a collagen component of reticular fibers in elastic tissues such as skin, lung, and blood vessels (41). Additionally, all three collagen type 5 α-chain genes (Col5a1, Col5a2, and Col5a3) were reduced in the diabetic samples. Collagen type 5 typically forms heterotypic or mixed fibrils with collagens type 1 and type 3 (41).

Elastic fibers, composed of microfibrillar bundles with an inner core of crosslinked elastin, provide tissues such as the corpora cavernosa with resilience and deformability that allow repeated cycles of expansion and recoil. The array analysis revealed significantly reduced expression of several genes encoding microfibril and elastic fiber-associated molecules in

the diabetic cavernosum (Table 1). The genes for elastin (Eln) and fibrillin1 (Fbn1) were modestly downregulated. Fibrillin protein is a principal component of the elastin-associated microfibrillar bundles (see recent review [62]). Diabetes was associated with decreased Mfap2 (microfibrillar-associated protein2) and Bgn (biglycan) gene expression. Mfap2 encodes a protein that may be important in microfibril structural integrity, whereas biglycan protein can form a complex with both MFAP2 and elastin molecules (62). Chondroitin sulfate proteoglycan2 (Cspg2; alias versican), with 2 to 3-fold reduced gene expression in diabetic samples, binds fibrillin molecules and may act to link elastin-associated microfibrils with surrounding ECM components in tissue (55). Interestingly, Cspg2 overexpression in cultured aortic SMCs increased elastin mRNA levels and induced elastic fiber formation (79). Merrilees and colleagues also showed that Cspg2 overexpression promotes elastic fiber deposition in balloon-injured rat carotid arteries (79).

The observed decline in diabetic gene expression of lysyl oxidase (Lox) is noteworthy considering Lox encodes an enzyme required for proper crosslinking of elastin and collagen in vascular tissue (50, 75). LOX crosslinking activity mediates stabilization of collagen and elastin fibers in the ECM and also helps deposit elastin onto microfibrils (58). In fact, arteries of Lox knockout mice show considerable structural alterations including fragmented elastic fibers (50, 75). Interestingly, low density lipoprotein (LDL) decreases Lox mRNA in cultured aortic endothelial cells, and hypercholesterolemia is associated with downregulation of Lox expression in aortic tissue (100). Lox mRNA is detected in both endothelial and smooth muscle cells *in vitro* and so multiple sources of LOX are likely in the cavernosum (100, 109). The levels of LOX or perhaps even the related LOX-like proteins (i.e., LOXL1 - LOXL4) may be important in cavernosal biology that is particularly related to ECM assembly, maintenance, and remodeling.

Previous studies evaluating human cavernosal structures show reduced elastic fibers in samples from impotent versus potent patients and diabetic versus non-diabetic patients (105, 128). Similar evaluations of elastic fibers in erectile tissue using animal models of diabetes have not been reported. Salama and colleagues (102) describe thickening of collagen bundles in the diabetic rat tunica albuginea and altered collagen architecture, but changes in elastic fibers were not addressed. Interestingly, the tunica albuginea of aged rats shows structural alterations including thinning and fragmentation of elastic fibers (15). These observations are consistent with studies of the vasculature showing that diabetes is associated with reduced elasticity of coronary arteries and decreased elastin levels in the aorta (68, 112).

Another notable finding is the reduced expression of Sparc (alias osteonectin), Spp1 (alias osteopontin), and Tnc (tenascin C) in the cavernosum of diabetic rats. Each of these genes encodes a member of the matricellular family of proteins. Matricellular proteins are unique ECM molecules that do not appear to have direct structural roles, but instead mediate cell-matrix interaction and cell function. For instance, Spp1 and Sparc are reported to influence diverse biological processes including vascular function and structure (refer to Table 2). Carotid arteries of Spp1 knockout mice exhibit loosely organized collagen fibers and vessels have increased compliance (81). Similarly, matrix disorganization and smaller diameter collagen fibrils are observed in the healing wounds of Spp1 knockouts (71). Sparc knockout mice also have phenotypes involving alterations in ECM organization and structure. For example, collagen fibers surrounding tumors grown in Sparc knockouts have reduced fiber diameter and attenuated fiber crosslinking (13). The dermis of mice lacking Sparc has decreased collagen fibril size and altered collagen composition, suggesting the presence of immature collagen fibers (12). It remains to be determined whether reduced matricellular protein expression in the diabetic cavernosum is causing alterations in ECM production and/or assembly.

Ceruloplasmin upregulation in the diabetic cavernosum

As explained in the results, we used PubMatrix searches of the differentially expressed genes to help identify molecules that might influence erectile responses by altering vascular function. Ceruloplasmin is an example of one such molecule previously shown to affect vascular responses. CP is a multifunctional protein, initially isolated from plasma, which has numerous proposed biological functions including copper transport, iron metabolism, and substrate oxidation and reduction (10). Alternative splicing of the Cp gene yields two distinct mRNA sequences that encode GPI-linked (membrane anchored) and secreted forms of CP, both of which were upregulated in the diabetic cavernosum based on real-time PCR (89). This is consistent with a recent study showing increased Cp gene expression (3.1-fold, Affymetrix data) and elevated CP protein (1.7-fold) in retinal cells from STZ-treated rats (42). Previous studies report increased serum CP levels in patients with type 1 or type 2 diabetes (22, 23).

Cp is expressed in numerous tissues including liver, testis, lung, brain, placenta, and eye (3, 65). Vascular SMCs grown *in vitro* express Cp mRNA (19) as do cultured SMCs derived from human cavernosal tissue (author's observation, data not shown). Strong CP antibody labeling of cavernosal SMCs is consistent with the idea that SMCs are the primary source of Cp gene and protein expression in our samples. Previous examinations of liver and lung tissue showed lack of Cp mRNA in the vascular endothelium, making it unlikely that cavernosal endothelial cells are a source of CP (65). However, liver endothelial cells are able to bind and internalize CP from the serum, possibly through interaction with a membrane receptor (59, 115). Therefore, CP localized to the cavernosal endothelium (Figure 3c and 3e) could be from the binding of CP produced locally (e.g., SMCs) and/or secreted by the liver (i.e., circulating in blood). The 16-fold upregulation of Cp-serum mRNA in diabetic samples seems to suggest that CP secretion may be enhanced locally within the erectile tissues. The Cp-GPI splice variant was also upregulated by diabetes (2.4 fold); based on mRNA abundance, this variant appears to be the principal form of Cp mRNA normally expressed in the cavernosum. Interestingly, GPI-anchored proteins exhibit cell to cell transfer in certain experimental conditions (67). Regardless of the source or form, higher amounts of CP protein were detected in the penile tissues of diabetic rats and the most prominent CP staining was localized to the cavernosal SMCs and endothelium.

In terms of vascular function, CP at physiological levels impairs endothelial-dependent relaxation of the aorta in a dose-dependent manner (17). This reduced vascular reactivity appears to be due to the ability of CP to decrease endothelial-dependent nitric oxide production via inhibition of eNOS (9). These activities may be related to enhanced copper (Cu^{2+}) transfer to vascular cells given that CP mediates the transfer of Cu^{2+} across cell membranes and that Cu^{2+} loading is observed in CP-treated endothelial cells (9, 92). Interestingly, Cu^{2+} and other divalent transition metals have direct inhibitory effects on neuronal NOS activity through direct binding of metal ions to the NOS enzyme (93, 94). Thus, CP and/or CP-derived Cu^{2+} ions can inhibit the two primary sources of NO required for penile erection (nNOS and eNOS). Additionally, CP has the ability to catalyze oxidation of NO to highly reactive nitrosonium (NO^{+}), which may directly alter NO bioavailability in the penis (10). Future studies are required to determine whether the association between Cp expression and erectile function is causal.

Lipoprotein lipase expression

According to the Resolver analysis and real-time PCR, Lpl gene expression was upregulated nearly 3-fold in the diabetic penile tissue. Previous reports of changes in Lpl expression in diabetic animals are variable depending on the type of tissue examined (25, 103, 114). Lpl encodes lipoprotein lipase, which is expressed in multiple tissues including heart, muscle,

adipose tissue, and vascular smooth muscle. LPL has the enzymatic function of triglyceride hydrolase and the non-enzymatic role of ligand/bridging factor for lipoprotein uptake. In the vasculature, SMCs are positive for Lpl mRNA and protein whereas endothelial cells have only LPL protein (16, 57). Immunofluorescence of control and diabetic cavernosal tissue showed strong LPL localization in the cavernosal sinusoids and adjacent vessels (online supplement, Figure II).

Transgenic mice overexpressing human Lpl in vascular smooth muscle have augmented contractile responses and reduced endothelial-dependent relaxation in the aorta (27). The aortas from these transgenic Lpl mice have increased levels of free fatty acids (FFA). This suggests that LPL within vessels acts to liberate FFAs that can then be taken up by vascular cells. FFA overloading in smooth muscle and endothelial cells can enhance the generation of reactive oxygen species, which reduces the production and the bioavailability of NO (28, 53). Also, LPL activity may alter vascular function by increasing cellular uptake of modified-LDLs (e.g., oxidized-LDL and glycated-LDL) by SMCs and endothelial cells (6, 80, 86, 131). Ox-LDL can impair both vascular and cavernosal relaxation, while glycated-LDL has been shown to induce endothelial cell apoptosis and reduce eNOS expression (1, 5, 107). These studies present multiple mechanisms by which cavernosal upregulation of Lpl could contribute to ED.

Cd36 expression

The 2-fold upregulation of Cd36 gene expression in the diabetic cavernosum is consistent with previous studies demonstrating increased CD36 in the heart of diabetic mice and tissues from diabetic rats (45, 90). Interestingly, macrophage Cd36 gene expression is increased by glucose and atherosclerotic lesions from patients with hyperglycemia have greater CD36 levels (46). CD36 (also termed fatty acid translocase) is a type B scavenger receptor that binds to collagen, thrombospondin, anionic phospholipids, and ox-LDL (see review [82]). CD36 is expressed by a variety of cell types including cardiac myocytes, skeletal myocytes, microvessel endothelial cells, and cultured aortic smooth muscle cells (45, 60, 99, 113). Immunostaining for CD36 in diabetic and control rat cavernosum showed strongest staining in capillaries and microvessels surrounding and within the erectile tissues, as well as discontinuous staining of the cavernosal sinusoids (online supplement, Figure III).

Studies of mutant mice have established a physiological role of CD36 in fatty acid and lipoprotein metabolism (32). Cd36 deficient cells show decreased binding and uptake of ox-LDL. In cultured aortic smooth muscle cells, CD36 mediates the cellular internalization of ox-LDL (99). In apoE/Cd36 double knockouts, the loss of CD36 is associated with reduced atherosclerotic lesion formation and preserved endothelial-dependent vessel responses (33, 64). The presence of CD36 in hypercholesterolemic apoE null mice alters eNOS localization which then impairs nitric oxide production (64). Increased CD36 levels in the penis could adversely affect cavernosal relaxation through mechanisms involving ox-LDL uptake and/or direct interaction with eNOS.

Smooth muscle cell biology and phenotype

Vascular SMCs show evidence of a spectrum of differentiated phenotypes and adult SMCs are capable of dynamic shifts in phenotype depending on local signals such as growth factors, matrix interactions, inflammatory stimuli, and hemodynamic forces (reviewed in [88]). Importantly, diabetes is a condition that induces phenotypic modulation of SMCs as evidenced by the expression of embryonic forms of matrix and contractile genes in the aortas of diabetic rats (37). In culture, SMCs isolated from diabetic animals have increased growth rates, altered contractile protein expression, and different ultrastructural organization compared to non-diabetic SMCs (29). Similarly, SMCs derived from vessels of diabetic

patients display phenotypic differences, including increased proliferation and migration as well as distinct cell morphology (31). Given that 1) diabetes alters SMC phenotype, 2) erectile tissues are specialized SMC-enriched vascular structures, and 3) normal SMC function is prerequisite for proper erectile activity; we sought to identify those differentially expressed genes in the diabetic samples with potential to impact SMC biology and phenotype.

The increased diabetic expression of transcription factors from the Kruppel-like factor family (Klf5 and Klf15, increased 3-fold and 2-fold, respectively) could be indicative of alterations in SMC phenotype. Klf5 (alias BTEB2) is expressed in the medial SMC layer of neonatal aorta but not in adult aorta (122). Also, Klf5 upregulation is localized to the intimal SMCs of restenotic lesions and injured vessels, suggesting that Klf5 plays a role in phenotypic modulation of SMCs in vascular disease (51, 122). Specifically, it appears that Klf5 acts as a transcriptional regulator of Myh10 (aliases SMemb and NM myosin heavy chain IIB) expression in SMCs which is indicative of a dedifferentiated, proliferative SMC phenotype (122). While Myh10 was unchanged in our study, we observed upregulation of the related gene Myh9 (myosin, heavy polypeptide9; alias non-muscle myosin heavy chain IIA) in diabetic cavernosal tissues (2-fold increase, $p = 0.0008$). Myh9 expression is detected in primary and restenotic atherosclerotic lesions (84). Additionally, MYH9 protein levels increased progressively in the vessel media and neointima following carotid injury in rats (38). The role of Klf15 in SMC biology has not been studied and so the significance of its upregulation in the diabetic cavernosum is unknown. Klf15 expression is present in all muscle lineages, including SMCs of the vasculature (44).

In relation to SMC phenotype, it is important to point out that we did not detect diabetes-associated changes in several SMC differentiation marker genes (e.g., Acta2-SMA α-actin; Myh11-SM myosin heavy chain; Cnn1-Calponin1; and Smtn-Smoothelin). This would seem to contradict the presence of profound or widespread dedifferentiation of SMCs in the diabetic cavernosum. However, previous array analysis of vascular neointima formation- characterized by SMC phenotypic modulation and proliferation- did not demonstrate wholesale changes in the above mentioned SMC markers (39). Also, we cannot rule out changes in expression of the various SMC genes at times other than our 10 week end-point or that alterations were present at the protein but not the mRNA level.

Based on literature mining, we were able to identify additional genes that could be affecting SMC biology in the diabetic rat penis. For example, diabetic upregulation of C3 (complement component3; 2-fold increase, $p = 0.00345$) may alter cavernosal SMC tone given that C3 is able to cause constriction of isolated arteries (77). C3 expression was detected selectively in the aorta and cultured SMCs from spontaneously hypertensive rats (72). Further, exogenous C3 protein caused dedifferentiation of SMCs and shifted gene expression towards a synthetic SMC phenotype (72). Another upregulated gene in the diabetic cavernosum, Cx3cl1 (chemokine C-X3-C motif ligand1; alias fractalkine) encodes a protein that is able to increase SMC adhesion and proliferation in an autocrine fashion in response to inflammatory cytokines (18). Cx3cl1 mRNA and protein are upregulated in diabetic rat kidneys as well as in atherosclerotic arteries from patients with and without diabetes (63, 127). Finally, we detected significantly reduced gene expression for S100a4 (alias metastasin and calvasculin), which encodes a member of the S100 family of $Ca2^{+}$-binding proteins. S100a4 has been implicated in various cellular processes and appears to be constitutively expressed in the aorta and cultured SMCs (24). Cellular localization of S100A4 protein in SMCs and vascular tissue shows S100A4 to be strongly associated with actin stress fibers and with the sarcoplasmic reticulum (76). In addition to interacting with intracellular proteins, S100A4 may have extracellular function as a secreted protein (124).

The potential for phenotypic modulation of the diabetic cavernosal smooth muscle is an intriguing idea that has yet to be established. Changes in any number of the above genes may be indicative of an altered differentiation/maturation state in the SMCs of the cavernosum and penile vasculature which would have important implications on erectile function. Phenotypic modulation may well reflect changes in the assortment of necessary contractile proteins, signaling molecules, growth factors, and matrix modulators of properly functioning cavernosal SMCs.

Limitations

Expression analysis with microarrays can be a valuable and powerful technique, but certain limitations exist in the present study that merit discussion. Although erectile tissues are relatively SMC-enriched, there is clearly a mixture of cell types in the harvested cavernosal samples. As a result, all the various cell types potentially contribute to the differential gene expression detected in this analysis. With the exception of certain cell-type specific genes, further characterization will be required to identify a particular source of altered gene expression. Additionally, our analysis merely establishes an association between the observed gene changes and diabetic ED. Further experimentation is necessary to distinguish between differentially expressed genes that are actual mediators of ED, markers of ED, or inconsequential to ED. This is an expected challenge often present in microarray studies and so our analysis should be primarily viewed as hypothesis generating. Also, the Affymetrix RAE 230A GeneChips contain probe sets representing over 15,000 genes and transcripts including the majority of full-length, well-annotated rat genes. However, the 230A GeneChip does not contain probe sets for all rat genes and as a result this analysis is incomplete. Furthermore, evaluation of gene expression at a single time point may miss critical changes that occur earlier or later in the progression of ED. A more comprehensive analysis of temporal changes, based on patterns of expression over time, would also be helpful in delineating those genes that might directly lead to ED. However, the high costs of evaluating large-scale gene expression (e.g., GeneChips) restricted the design of our current study. Related to this, we were not able to examine gene expression patterns from multiple organs or tissues which may be a useful strategy to differentiate between global versus tissue-specific expression changes in response to diabetes. By surveying expression patterns across several tissues, Knoll and colleagues to were able to identify common and tissue-specific transcriptional changes in response to short-term diabetes in rats (66). Finally, while Gene Ontology analysis is reasonably objective in design, we acknowledge that literature mining as it was used here is a rather subjective method to identify genes of interest. Nevertheless, PubMatrix was a useful tool to generate a vascular-focused and disease-relevant annotation of our microarray data. We think that such an approach is appropriate given the vascular nature of erectile tissue and the physiology of penile erection. The availability of the raw Affymetrix files in the GEO repository will allow other researchers to apply different data-mining strategies and analysis techniques to our data. Also, future analysis combining data sets from other research groups using microarrays to study erectile dysfunction may be useful to identify common mechanisms present in the different animal models of ED (119).

Summary

This study expands the scope of potential candidate genes and pathways that are dysregulated by diabetes and that could negatively impact erectile function. Based on Gene Ontology classification, there was an enrichment of dysregulated extracellular matrix genes (e.g., collagen and elastin related) that may have important functions related to cavernosal structure (e.g., lysyl oxidase). Also, we have focused on the discovery of novel gene changes that may affect the proper function of vascular cells in the penis (e.g., ceruloplasmin) and therefore contribute the development of ED. The various genes and molecules that have

been identified in our study can be further evaluated as possible diagnostic tools (e.g., biomarkers) or potential drug targets in patients with diabetes-associated ED.

Supplementary Material

Refer to Web version on PubMed Central for supplementary material.

Acknowledgments

Funding

NIH 1RO1DK55017, 5T32DK007779, 5U24DK058813

Refrences

1. Ahn TY, Gomez-Coronado D, Martinez V, Cuevas P, Goldstein I, Saenz dTI. Enhanced contractility of rabbit corpus cavernosum smooth muscle by oxidized low density lipoproteins. Int J Impot Res. 1999; 11:9–14. [PubMed: 10098947]
2. Akimoto Y, Kreppel LK, Hirano H, Hart GW. Hyperglycemia and the O-GlcNAc transferase in rat aortic smooth muscle cells: elevated expression and altered patterns of O-GlcNAcylation. Arch Biochem Biophys. 2001; 389:166–175. [PubMed: 11339805]
3. Aldred AR, Grimes A, Schreiber G, Mercer JF. Rat ceruloplasmin. Molecular cloning and gene expression in liver, choroid plexus, yolk sac, placenta, and testis. J Biol Chem. 1987; 262:2875–2878. [PubMed: 3818625]
4. Andersson KE. Erectile physiological and pathophysiological pathways involved in erectile dysfunction. J Urol. 2003; 170:S6–S13. [PubMed: 12853766]
5. Artwohl M, Graier WF, Roden M, Bischof M, Freudenthaler A, Waldhausl W, Baumgartner-Parzer SM. Diabetic LDL triggers apoptosis in vascular endothelial cells. Diabetes. 2003; 52:1240–1247. [PubMed: 12716759]
6. Auerbach BJ, Bisgaier CL, Wolle J, Saxena U. Oxidation of low density lipoproteins greatly enhances their association with lipoprotein lipase anchored to endothelial cell matrix. J Biol Chem. 1996; 271:1329–1335. [PubMed: 8576120]
7. Basu A, Ryder RE. New treatment options for erectile dysfunction in patients with diabetes mellitus. Drugs. 2004; 64:2667–2688. [PubMed: 15537369]
8. Becker KG, Hosack DA, Dennis G Jr, Lempicki RA, Bright TJ, Cheadle C, Engel J. PubMatrix: a tool for multiplex literature mining. BMC Bioinformatics. 2003; 4:61. [PubMed: 14667255]
9. Bianchini A, Musci G, Calabrese L. Inhibition of endothelial nitric-oxide synthase by ceruloplasmin. J Biol Chem. 1999; 274:20265–20270. [PubMed: 10400645]
10. Bielli P, Calabrese L. Structure to function relationships in ceruloplasmin: a 'moonlighting' protein. Cell Mol Life Sci. 2002; 59:1413–1427. [PubMed: 12440766]
11. Bivalacqua TJ, Usta MF, Champion HC, Kadowitz PJ, Hellstrom WJ. Endothelial dysfunction in erectile dysfunction: role of the endothelium in erectile physiology and disease. J Androl. 2003; 24:S17–S37. [PubMed: 14581492]
12. Bradshaw AD, Puolakkainen P, Dasgupta J, Davidson JM, Wight TN, Helene SE. SPARC-null mice display abnormalities in the dermis characterized by decreased collagen fibril diameter and reduced tensile strength. J Invest Dermatol. 2003; 120:949–955. [PubMed: 12787119]
13. Brekken RA, Puolakkainen P, Graves DC, Workman G, Lubkin SR, Sage EH. Enhanced growth of tumors in SPARC null mice is associated with changes in the ECM. J Clin Invest. 2003; 111:487–495. [PubMed: 12588887]
14. Brown JS, Wessells H, Chancellor MB, Howards SS, Stamm WE, Stapleton AE, Steers WD, Van Den Eeden SK, McVary KT. Urologic complications of diabetes. Diabetes Care. 2005; 28:177–185. [PubMed: 15616253]

15. Calabro A, Italiano G, Pescatori ES, Marin A, Gaetano O, Abatangelo G, Abatangelo G, Pagano F. Physiological aging and penile erectile function: a study in the rat. Eur Urol. 1996; 29:240–244. [PubMed: 8647156]

16. Camps L, Reina M, Llobera M, Vilaro S, Olivecrona T. Lipoprotein lipase: cellular origin and functional distribution. Am J Physiol. 1990; 258:C673–C681. [PubMed: 2185641]

17. Cappelli-Bigazzi M, Ambrosio G, Musci G, Battaglia C, Bonaccorsi di Patti MC, Golino P, Ragni M, Chiariello M, Calabrese L. Ceruloplasmin impairs endothelium-dependent relaxation of rabbit aorta. Am J Physiol. 1997; 273:H2843–H2849. [PubMed: 9435622]

18. Chandrasekar B, Mummidi S, Perla RP, Bysani S, Dulin NO, Liu F, Melby PC. Fractalkine (CX3CL1) stimulated by nuclear factor kappaB (NF-kappaB)-dependent inflammatory signals induces aortic smooth muscle cell proliferation through an autocrine pathway. Biochem J. 2003; 373:547–558. [PubMed: 12729461]

19. Chen J, Maltby KM, Miano JM. A novel retinoid-response gene set in vascular smooth muscle cells. Biochem Biophys Res Commun. 2001; 281:475–482. [PubMed: 11181072]

20. Chen L, Dentchev T, Wong R, Hahn P, Wen R, Bennett J, Dunaief JL. Increased expression of ceruloplasmin in the retina following photic injury. Mol Vis. 2003; 9:151–158. [PubMed: 12724641]

21. Conti G, Virag R. Human penile erection and organic impotence: normal histology and histopathology. Urol Int. 1989; 44:303–308. [PubMed: 2800066]

22. Cunningham J, Leffell M, Mearkle P, Harmatz P. Elevated plasma ceruloplasmin in insulin-dependent diabetes mellitus: evidence for increased oxidative stress as a variable complication. Metabolism. 1995; 44:996–999. [PubMed: 7637657]

23. Daimon M, Susa S, Yamatani K, Manaka H, Hama K, Kimura M, Ohnuma H, Kato T. Hyperglycemia is a factor for an increase in serum ceruloplasmin in type 2 diabetes. Diabetes Care. 1998; 21:1525–1528. [PubMed: 9727903]

24. Daub B, Schroeter M, Pfitzer G, Ganitkevich V. Expression of members of the S100 Ca2+-binding protein family in guinea-pig smooth muscle. Cell Calcium. 2003; 33:1–10. [PubMed: 12526882]

25. de FV, Neubauer H, Poussin C, Farmer P, Falquet L, Burcelin R, Delorenzi M, Thorens B. Transcript profiling suggests that differential metabolic adaptation of mice to a high fat diet is associated with changes in liver to muscle lipid fluxes. J Biol Chem. 2004; 279:50743–50753. [PubMed: 15377667]

26. El Sakka AI, Lin CS, Chui RM, Dahiya R, Lue TF. Effects of diabetes on nitric oxide synthase and growth factor genes and protein expression in an animal model. Int J Impot Res. 1999; 11:123–132. [PubMed: 10404280]

27. Esenabhalu VE, Cerimagic M, Malli R, Osibow K, Levak-Frank S, Frieden M, Sattler W, Kostner GM, Zechner R, Graier WF. Tissue-specific expression of human lipoprotein lipase in the vascular system affects vascular reactivity in transgenic mice. Br J Pharmacol. 2002; 135:143–154. [PubMed: 11786490]

28. Esenabhalu VE, Schaeffer G, Graier WF. Free fatty acid overload attenuates Ca2+ signaling and NO production in endothelial cells. Antioxid Redox Signal. 2003; 5:147–153. [PubMed: 12716474]

29. Etienne P, Pares-Herbute N, Mani-Ponset L, Gabrion J, Rabesandratana H, Herbute S, Monnier L. Phenotype modulation in primary cultures of aortic smooth muscle cells from streptozotocin-diabetic rats. Differentiation. 1998; 63:225–236. [PubMed: 9745713]

30. Fani K, Lundin AP, Beyer MM, Jimenez FA, Friedman EA. Pathology of the penis in long-term diabetic rats. Diabetologia. 1983; 25:424–428. [PubMed: 6606592]

31. Faries PL, Rohan DI, Takahara H, Wyers MC, Contreras MA, Quist WC, King GL, Logerfo FW. Human vascular smooth muscle cells of diabetic origin exhibit increased proliferation, adhesion, and migration. J Vasc Surg. 2001; 33:601–607. [PubMed: 11241133]

32. Febbraio M, Abumrad NA, Hajjar DP, Sharma K, Cheng W, Pearce SF, Silverstein RL. A null mutation in murine CD36 reveals an important role in fatty acid and lipoprotein metabolism. J Biol Chem. 1999; 274:19055–19062. [PubMed: 10383407]

33. Febbraio M, Podrez EA, Smith JD, Hajjar DP, Hazen SL, Hoff HF, Sharma K, Silverstein RL. Targeted disruption of the class B scavenger receptor CD36 protects against atherosclerotic lesion development in mice. J Clin Invest. 2000; 105:1049–1056. [PubMed: 10772649]
34. Feldman HA, Goldstein I, Hatzichristou DG, Krane RJ, McKinlay JB. Impotence and its medical and psychosocial correlates: results of the Massachusetts Male Aging Study. J Urol. 1994; 151:54–61. [PubMed: 8254833]
35. Fiore R, Puschel AW. The function of semaphorins during nervous system development. Front Biosci. 2003; 8:s484–s499. [PubMed: 12700098]
36. Freedman SJ, Sun ZY, Kung AL, France DS, Wagner G, Eck MJ. Structural basis for negative regulation of hypoxia-inducible factor-1alpha by CITED2. Nat Struct Biol. 2003; 10:504–512. [PubMed: 12778114]
37. Fukuda G, Khan ZA, Barbin YP, Farhangkhoee H, Tilton RG, Chakrabarti S. Endothelin-mediated remodeling in aortas of diabetic rats. Diabetes Metab Res Rev. 2004
38. Gallagher PJ, Jin Y, Killough G, Blue EK, Lindner V. Alterations in expression of myosin and myosin light chain kinases in response to vascular injury. Am J Physiol Cell Physiol. 2000; 279:C1078–C1087. [PubMed: 11003588]
39. Geary RL, Wong JM, Rossini A, Schwartz SM, Adams LD. Expression profiling identifies 147 genes contributing to a unique primate neointimal smooth muscle cell phenotype. Arterioscler Thromb Vasc Biol. 2002; 22:2010–2016. [PubMed: 12482827]
40. Gefen A, Chen J, Elad D. Computational tools in rehabilitation of erectile dysfunction. Med Eng Phys. 2001; 23:69–82. [PubMed: 11413059]
41. Gelse K, Poschl E, Aigner T. Collagens--structure, function, and biosynthesis. Adv Drug Deliv Rev. 2003; 55:1531–1546. [PubMed: 14623400]
42. Gerhardinger C, Costa MB, Coulombe MC, Toth I, Hoehn T, Grosu P. Expression of acute-phase response proteins in retinal muller cells in diabetes. Invest Ophthalmol Vis Sci. 2005; 46:349–357. [PubMed: 15623795]
43. Goulas A, Papakonstantinou E, Karakiulakis G, Mirtsou-Fidani V, Kalinderis A, Hatzichristou DG. Tissue structure-specific distribution of glycosaminoglycans in the human penis. Int J Biochem Cell Biol. 2000; 32:975–982. [PubMed: 11084377]
44. Gray S, Feinberg MW, Hull S, Kuo CT, Watanabe M, Sen-Banerjee S, DePina A, Haspel R, Jain MK. The Kruppel-like factor KLF15 regulates the insulin-sensitive glucose transporter GLUT4. J Biol Chem. 2002; 277:34322–34328. [PubMed: 12097321]
45. Greenwalt DE, Scheck SH, Rhinehart-Jones T. Heart CD36 expression is increased in murine models of diabetes and in mice fed a high fat diet. J Clin Invest. 1995; 96:1382–1388. [PubMed: 7544802]
46. Griffin E, Re A, Hamel N, Fu C, Bush H, McCaffrey T, Asch AS. A link between diabetes and atherosclerosis: Glucose regulates expression of CD36 at the level of translation. Nat Med. 2001; 7:840–846. [PubMed: 11433350]
47. Guay AT, Perez JB, Jacobson J, Newton RA. Efficacy and safety of sildenafil citrate for treatment of erectile dysfunction in a population with associated organic risk factors. J Androl. 2001; 22:793–797. [PubMed: 11545291]
48. Guy PM, Kenny DA, Gill GN. The PDZ domain of the LIM protein enigma binds to beta-tropomyosin. Mol Biol Cell. 1999; 10:1973–1984. [PubMed: 10359609]
49. Hedlund P, Aszodi A, Pfeifer A, Alm P, Hofmann F, Ahmad M, Fassler R, Andersson KE. Erectile dysfunction in cyclic GMP-dependent kinase I-deficient mice. Proc Natl Acad Sci U S A. 2000; 97:2349–2354. [PubMed: 10688876]
50. Hornstra IK, Birge S, Starcher B, Bailey AJ, Mecham RP, Shapiro SD. Lysyl oxidase is required for vascular and diaphragmatic development in mice. J Biol Chem. 2003; 278:14387–14393. [PubMed: 12473682]
51. Hoshino Y, Kurabayashi M, Kanda T, Hasegawa A, Sakamoto H, Okamoto E, Kowase K, Watanabe N, Manabe I, Suzuki T, Nakano A, Takase S, Wilcox JN, Nagai R. Regulated expression of the BTEB2 transcription factor in vascular smooth muscle cells: analysis of developmental and pathological expression profiles shows implications as a predictive factor for restenosis. Circulation. 2000; 102:2528–2534. [PubMed: 11076828]

52. Hsu GL, Brock G, von Heyden B, Nunes L, Lue TF, Tanagho EA. The distribution of elastic fibrous elements within the human penis. Br J Urol. 1994; 73:566–571. [PubMed: 8012781]

53. Inoguchi T, Li P, Umeda F, Yu HY, Kakimoto M, Imamura M, Aoki T, Etoh T, Hashimoto T, Naruse M, Sano H, Utsumi H, Nawata H. High glucose level and free fatty acid stimulate reactive oxygen species production through protein kinase C--dependent activation of NAD(P)H oxidase in cultured vascular cells. Diabetes. 2000; 49:1939–1945. [PubMed: 11078463]

54. Inohara N, Koseki T, Chen S, Wu X, Nunez G. CIDE, a novel family of cell death activators with homology to the 45 kDa subunit of the DNA fragmentation factor. EMBO J. 1998; 17:2526–2533. [PubMed: 9564035]

55. Isogai Z, Aspberg A, Keene DR, Ono RN, Reinhardt DP, Sakai LY. Versican interacts with fibrillin-1 and links extracellular microfibrils to other connective tissue networks. J Biol Chem. 2002; 277:4565–4572. [PubMed: 11726670]

56. Jeays-Ward K, Hoyle C, Brennan J, Dandonneau M, Alldus G, Capel B, Swain A. Endothelial and steroidogenic cell migration are regulated by WNT4 in the developing mammalian gonad. Development. 2003; 130:3663–3670. [PubMed: 12835383]

57. Jonasson L, Bondjers G, Hansson GK. Lipoprotein lipase in atherosclerosis: its presence in smooth muscle cells and absence from macrophages. J Lipid Res. 1987; 28:437–445. [PubMed: 3585176]

58. Kagan HM, Vaccaro CA, Bronson RE, Tang SS, Brody JS. Ultrastructural immunolocalization of lysyl oxidase in vascular connective tissue. J Cell Biol. 1986; 103:1121–1128. [PubMed: 2875077]

59. Kataoka M, Tavassoli M. Ceruloplasmin receptors in liver cell suspensions are limited to the endothelium. Exp Cell Res. 1984; 155:232–240. [PubMed: 6092118]

60. Keizer HA, Schaart G, Tandon NN, Glatz JF, Luiken JJ. Subcellular immunolocalisation of fatty acid translocase (FAT)/CD36 in human type-1 and type-2 skeletal muscle fibres. Histochem Cell Biol. 2004; 121:101–107. [PubMed: 14740222]

61. Khokha MK, Hsu D, Brunet LJ, Dionne MS, Harland RM. Gremlin is the BMP antagonist required for maintenance of Shh and Fgf signals during limb patterning. Nat Genet. 2003; 34:303–307. [PubMed: 12808456]

62. Kielty CM, Sherratt MJ, Shuttleworth CA. Elastic fibres. J Cell Sci. 2002; 115:2817–2828. [PubMed: 12082143]

63. Kikuchi Y, Ikee R, Hemmi N, Hyodo N, Saigusa T, Namikoshi T, Yamada M, Suzuki S, Miura S. Fractalkine and its receptor, CX3CR1, upregulation in streptozotocin-induced diabetic kidneys. Nephron Exp Nephrol. 2004; 97:e17–e25. [PubMed: 15153757]

64. Kincer JF, Uittenbogaard A, Dressman J, Guerin TM, Febbraio M, Guo L, Smart EJ. Hypercholesterolemia promotes a CD36-dependent and endothelial nitric-oxide synthase-mediated vascular dysfunction. J Biol Chem. 2002; 277:23525–23533. [PubMed: 11976335]

65. Klomp LW, Farhangrazi ZS, Dugan LL, Gitlin JD. Ceruloplasmin gene expression in the murine central nervous system. J Clin Invest. 1996; 98:207–215. [PubMed: 8690795]

66. Knoll KE, Pietrusz JL, Liang M. Tissue-specific transcriptome responses in rats with early streptozotocin-induced diabetes. Physiol Genomics. 2005; 21:222–229. [PubMed: 15713786]

67. Kooyman DL, Byrne GW, McClellan S, Nielsen D, Tone M, Waldmann H, Coffman TM, McCurry KR, Platt JL, Logan JS. In vivo transfer of GPI-linked complement restriction factors from erythrocytes to the endothelium. Science. 1995; 269:89–92. [PubMed: 7541557]

68. Kwan CY, Wang RR, Beazley JS, Lee RM. Alterations of elastin and elastase-like activities in aortae of diabetic rats. Biochim Biophys Acta. 1988; 967:322–325. [PubMed: 3191158]

69. Labus MB, Stirk CM, Thompson WD, Melvin WT. Expression of Wnt genes in early wound healing. Wound Repair Regen. 1998; 6:58–64. [PubMed: 9776851]

70. Lappin DW, McMahon R, Murphy M, Brady HR. Gremlin: an example of the re-emergence of developmental programmes in diabetic nephropathy. Nephrol Dial Transplant. 2002; 17(Suppl 9): 65–67. [PubMed: 12386293]

71. Liaw L, Birk DE, Ballas CB, Whitsitt JS, Davidson JM, Hogan BL. Altered wound healing in mice lacking a functional osteopontin gene (spp1). J Clin Invest. 1998; 101:1468–1478. [PubMed: 9525990]

72. Lin ZH, Fukuda N, Jin XQ, Yao EH, Ueno T, Endo M, Saito S, Matsumoto K, Mugishima H. Complement 3 is involved in the synthetic phenotype and exaggerated growth of vascular smooth

muscle cells from spontaneously hypertensive rats. Hypertension. 2004; 44:42–47. [PubMed: 15136559]

73. Livak KJ, Schmittgen TD. Analysis of relative gene expression data using real-time quantitative PCR and the 2(-Delta Delta C(T)) Method. Methods. 2001; 25:402–408. [PubMed: 11846609]
74. Luangkhot R, Rutchik S, Agarwal V, Puglia K, Bhargava G, Melman A. Collagen alterations in the corpus cavernosum of men with sexual dysfunction. J Urol. 1992; 148:467–471. [PubMed: 1635159]
75. Maki JM, Rasanen J, Tikkanen H, Sormunen R, Makikallio K, Kivirikko KI, Soininen R. Inactivation of the lysyl oxidase gene Lox leads to aortic aneurysms, cardiovascular dysfunction, and perinatal death in mice. Circulation. 2002; 106:2503–2509. [PubMed: 12417550]
76. Mandinova A, Atar D, Schafer BW, Spiess M, Aebi U, Heizmann CW. Distinct subcellular localization of calcium binding S100 proteins in human smooth muscle cells and their relocation in response to rises in intracellular calcium. J Cell Sci. 1998; 111(Pt 14):2043–2054. [PubMed: 9645951]
77. Marceau F, deBlois D, Laplante C, Petitclerc E, Pelletier G, Grose JH, Hugli TE. Contractile effect of the chemotactic factors f-Met-Leu-Phe and C5a on the human isolated umbilical artery. Role of cyclooxygenase products and tissue macrophages. Circ Res. 1990; 67:1059–1070. [PubMed: 1699682]
78. Meilhac O, Zhou M, Santanam N, Parthasarathy S. Lipid peroxides induce expression of catalase in cultured vascular cells. J Lipid Res. 2000; 41:1205–1213. [PubMed: 10946007]
79. Merrilees MJ, Lemire JM, Fischer JW, Kinsella MG, Braun KR, Clowes AW, Wight TN. Retrovirally mediated overexpression of versican v3 by arterial smooth muscle cells induces tropoelastin synthesis and elastic fiber formation in vitro and in neointima after vascular injury. Circ Res. 2002; 90:481–487. [PubMed: 11884379]
80. Mulder M, Lombardi P, Jansen H, van Berkel TJ, Frants RR, Havekes LM. Low density lipoprotein receptor internalizes low density and very low density lipoproteins that are bound to heparan sulfate proteoglycans via lipoprotein lipase. J Biol Chem. 1993; 268:9369–9375. [PubMed: 8387492]
81. Myers DL, Harmon KJ, Lindner V, Liaw L. Alterations of arterial physiology in osteopontin-null mice. Arterioscler Thromb Vasc Biol. 2003; 23:1021–1028. [PubMed: 12714436]
82. Nicholson AC, Han J, Febbraio M, Silversterin RL, Hajjar DP. Role of CD36, the macrophage class B scavenger receptor, in atherosclerosis. Ann N Y Acad Sci. 2001; 947:224–228. [PubMed: 11795270]
83. Nikkari ST, Jarvelainen HT, Wight TN, Ferguson M, Clowes AW. Smooth muscle cell expression of extracellular matrix genes after arterial injury. Am J Pathol. 1994; 144:1348–1356. [PubMed: 8203472]
84. Nikol S, Murakami N, Pickering JG, Kearney M, Leclerc G, Hofling B, Isner JM, Weir L. Differential expression of nonmuscle myosin II isoforms in human atherosclerotic plaque. Atherosclerosis. 1997; 130:71–85. [PubMed: 9126650]
85. Nuthakki VK, Fleser PS, Malinzak LE, Seymour ML, Callahan RE, Bendick PJ, Zelenock GB, Shanley CJ. Lysyl oxidase expression in a rat model of arterial balloon injury. J Vasc Surg. 2004; 40:123–129. [PubMed: 15218472]
86. Olin KL, Potter-Perigo S, Barrett PH, Wight TN, Chait A. Lipoprotein lipase enhances the binding of native and oxidized low density lipoproteins to versican and biglycan synthesized by cultured arterial smooth muscle cells. J Biol Chem. 1999; 274:34629–34636. [PubMed: 10574927]
87. Onichtchouk D, Chen YG, Dosch R, Gawantka V, Delius H, Massague J, Niehrs C. Silencing of TGF-beta signalling by the pseudoreceptor BAMBI. Nature. 1999; 401:480–485. [PubMed: 10519551]
88. Owens GK, Kumar MS, Wamhoff BR. Molecular regulation of vascular smooth muscle cell differentiation in development and disease. Physiol Rev. 2004; 84:767–801. [PubMed: 15269336]
89. Patel BN, Dunn RJ, David S. Alternative RNA splicing generates a glycosylphosphatidylinositol-anchored form of ceruloplasmin in mammalian brain. J Biol Chem. 2000; 275:4305–4310. [PubMed: 10660599]

90. Pelsers MM, Lutgerink JT, Nieuwenhoven FA, Tandon NN, van der Vusse GJ, Arends JW, Hoogenboom HR, Glatz JF. A sensitive immunoassay for rat fatty acid translocase (CD36) using phage antibodies selected on cell transfectants: abundant presence of fatty acid translocase/CD36 in cardiac and red skeletal muscle and up-regulation in diabetes. Biochem J. 1999; 337(Pt 3):407–414. [PubMed: 9895283]

91. Penson DF, Latini DM, Lubeck DP, Wallace KL, Henning JM, Lue TF. Do impotent men with diabetes have more severe erectile dysfunction and worse quality of life than the general population of impotent patients? Results from the Exploratory Comprehensive Evaluation of Erectile Dysfunction (ExCEED) database. Diabetes Care. 2003; 26:1093–1099. [PubMed: 12663579]

92. Percival SS, Harris ED. Copper transport from ceruloplasmin: characterization of the cellular uptake mechanism. Am J Physiol. 1990; 258:C140–C146. [PubMed: 2301561]

93. Perry JM, Marletta MA. Effects of transition metals on nitric oxide synthase catalysis. Proc Natl Acad Sci U S A. 1998; 95:11101–11106. [PubMed: 9736696]

94. Perry JM, Zhao Y, Marletta MA. Cu2+ and Zn2+ inhibit nitric-oxide synthase through an interaction with the reductase domain. J Biol Chem. 2000; 275:14070–14076. [PubMed: 10799481]

95. Persson C, Diederichs W, Lue TF, Yen TS, Fishman IJ, McLin PH, Tanagho EA. Correlation of altered penile ultrastructure with clinical arterial evaluation. J Urol. 1989; 142:1462–1468. [PubMed: 2685365]

96. Pinheiro AC, Costa WS, Cardoso LE, Sampaio FJ. Organization and relative content of smooth muscle cells, collagen and elastic fibers in the corpus cavernosum of rat penis. J Urol. 2000; 164:1802–1806. [PubMed: 11025773]

97. Rajagopalan D. A comparison of statistical methods for analysis of high density oligonucleotide array data. Bioinformatics. 2003; 19:1469–1476. [PubMed: 12912826]

98. Rehman J, Chenven E, Brink P, Peterson B, Walcott B, Wen YP, Melman A, Christ G. Diminished neurogenic but not pharmacological erections in the 2- to 3-month experimentally diabetic F-344 rat. Am J Physiol. 1997; 272:H1960–H1971. [PubMed: 9139984]

99. Ricciarelli R, Zingg JM, Azzi A. Vitamin E reduces the uptake of oxidized LDL by inhibiting CD36 scavenger receptor expression in cultured aortic smooth muscle cells. Circulation. 2000; 102:82–87. [PubMed: 10880419]

100. Rodriguez C, Raposo B, Martinez-Gonzalez J, Casani L, Badimon L. Low density lipoproteins downregulate lysyl oxidase in vascular endothelial cells and the arterial wall. Arterioscler Thromb Vasc Biol. 2002; 22:1409–1414. [PubMed: 12231558]

101. Rosen RC, Fisher WA, Eardley I, Niederberger C, Nadel A, Sand M. The multinational Men's Attitudes to Life Events and Sexuality (MALES) study: I. Prevalence of erectile dysfunction and related health concerns in the general population. Curr Med Res Opin. 2004; 20:607–617. [PubMed: 15171225]

102. Salama N, Kagawa S. Ultra-structural changes in collagen of penile tunica albuginea in aged and diabetic rats. Int J Impot Res. 1999; 11:99–105. [PubMed: 10356670]

103. Sambandam N, Abrahani MA, St Pierre E, Al Atar O, Cam MC, Rodrigues B. Localization of lipoprotein lipase in the diabetic heart: regulation by acute changes in insulin. Arterioscler Thromb Vasc Biol. 1999; 19:1526–1534. [PubMed: 10364085]

104. Santos CF, Caprio MA, Oliveira EB, Salgado MC, Schippers DN, Munzenmaier DH, Greene AS. Functional role, cellular source, and tissue distribution of rat elastase-2, an angiotensin II-forming enzyme. Am J Physiol Heart Circ Physiol. 2003; 285:H775–H783. [PubMed: 12714330]

105. Sattar AA, Wespes E, Schulman CC. Computerized measurement of penile elastic fibres in potent and impotent men. Eur Urol. 1994; 25:142–144. [PubMed: 8137855]

106. Shanahan CM, Cary NR, Salisbury JR, Proudfoot D, Weissberg PL, Edmonds ME. Medial localization of mineralization-regulating proteins in association with Monckeberg's sclerosis: evidence for smooth muscle cell-mediated vascular calcification. Circulation. 1999; 100:2168–2176. [PubMed: 10571976]

107. Simon BC, Cunningham LD, Cohen RA. Oxidized low density lipoproteins cause contraction and inhibit endothelium-dependent relaxation in the pig coronary artery. J Clin Invest. 1990; 86:75–79. [PubMed: 2365828]

108. Simonsen U, Garcia-Sacristan A, Prieto D. Penile arteries and erection. J Vasc Res. 2002; 39:283–303. [PubMed: 12187119]

109. Song YL, Ford JW, Gordon D, Shanley CJ. Regulation of lysyl oxidase by interferon-gamma in rat aortic smooth muscle cells. Arterioscler Thromb Vasc Biol. 2000; 20:982–988. [PubMed: 10764662]

110. Storey JD, Tibshirani R. Statistical significance for genomewide studies. Proc Natl Acad Sci U S A. 2003; 100:9440–9445. [PubMed: 12883005]

111. Surendran K, McCaul SP, Simon TC. A role for Wnt-4 in renal fibrosis. Am J Physiol Renal Physiol. 2002; 282:F431–F441. [PubMed: 11832423]

112. Tajaddini A, Kilpatrick DL, Schoenhagen P, Tuzcu EM, Lieber M, Vince DG. Impact of age and hyperglycemia on the mechanical behavior of intact human coronary arteries: an ex vivo intravascular ultrasound study. Am J Physiol Heart Circ Physiol. 2005; 288:H250–H255. [PubMed: 15331362]

113. Tanaka T, Kawamura K. Isolation of myocardial membrane long-chain fatty acid-binding protein: homology with a rat membrane protein implicated in the binding or transport of long-chain fatty acids. J Mol Cell Cardiol. 1995; 27:1613–1622. [PubMed: 8523424]

114. Tavangar K, Murata Y, Pedersen ME, Goers JF, Hoffman AR, Kraemer FB. Regulation of lipoprotein lipase in the diabetic rat. J Clin Invest. 1992; 90:1672–1678. [PubMed: 1430198]

115. Tavassoli M, Kishimoto T, Kataoka M. Liver endothelium mediates the hepatocyte's uptake of ceruloplasmin. J Cell Biol. 1986; 102:1298–1303. [PubMed: 3958047]

116. Tien ES, Davis JW, Vanden Heuvel JP. Identification of the CREB-binding protein/p300-interacting protein CITED2 as a peroxisome proliferator-activated receptor alpha coregulator. J Biol Chem. 2004; 279:24053–24063. [PubMed: 15051727]

117. Tsang M, Kim R, de Caestecker MP, Kudoh T, Roberts AB, Dawid IB. Zebrafish nma is involved in TGFbeta family signaling. Genesis. 2000; 28:47–57. [PubMed: 11064421]

118. Udelson D, Nehra A, Hatzichristou DG, Azadzoi K, Moreland RB, Krane J, Saenz dTI, Goldstein I. Engineering analysis of penile hemodynamic and structural-dynamic relationships: Part I--Clinical implications of penile tissue mechanical properties. Int J Impot Res. 1998; 10:15–24. [PubMed: 9542686]

119. User HM, Zelner DJ, McKenna KE, McVary KT. Microarray analysis and description of SMR1 gene in rat penis in a post-radical prostatectomy model of erectile dysfunction. J Urol. 2003; 170:298–301. [PubMed: 12796709]

120. Valks DM, Kemp TJ, Clerk A. Regulation of Bcl-xL expression by H2O2 in cardiac myocytes. J Biol Chem. 2003; 278:25542–25547. [PubMed: 12721309]

121. Wada T, McKee MD, Steitz S, Giachelli CM. Calcification of vascular smooth muscle cell cultures: inhibition by osteopontin. Circ Res. 1999; 84:166–178. [PubMed: 9933248]

122. Watanabe N, Kurabayashi M, Shimomura Y, Kawai-Kowase K, Hoshino Y, Manabe I, Watanabe M, Aikawa M, Kuro-o M, Suzuki T, Yazaki Y, Nagai R. BTEB2, a Kruppel-like transcription factor, regulates expression of the SMemb/Nonmuscle myosin heavy chain B (SMemb/NMHC-B) gene. Circ Res. 1999; 85:182–191. [PubMed: 10417400]

123. Watanabe T, Akishita M, Nakaoka T, He H, Miyahara Y, Yamashita N, Wada Y, Aburatani H, Yoshizumi M, Kozaki K, Ouchi Y. Caveolin-1, Id3a and two LIM protein genes are upregulated by estrogen in vascular smooth muscle cells. Life Sci. 2004; 75:1219–1229. [PubMed: 15219810]

124. Watanabe Y, Usuda N, Tsugane S, Kobayashi R, Hidaka H. Calvasculin, an encoded protein from mRNA termed pEL-98, 18A2, 42A, or p9Ka, is secreted by smooth muscle cells in culture and exhibits Ca(2+)-dependent binding to 36-kDa microfibril-associated glycoprotein. J Biol Chem. 1992; 267:17136–17140. [PubMed: 1512251]

125. Wessells H, Hruby VJ, Hackett J, Han G, Balse-Srinivasan P, Vanderah TW. AC-NLE-c[Asp-His-DPhe-Arg-Trp-Lys]-NH2 induces penile erection via brain and spinal melanocortin receptors. Neuroscience. 2003; 118:755–762. [PubMed: 12710982]

126. Wessells H, King SH, Schmelz M, Nagle RB, Heimark RL. Immunohistochemical comparison of vascular and sinusoidal adherens junctions in cavernosal endothelium. Urology. 2004; 63:201–206. [PubMed: 14751392]

127. Wong BW, Wong D, McManus BM. Characterization of fractalkine (CX3CL1) and CX3CR1 in human coronary arteries with native atherosclerosis, diabetes mellitus, and transplant vascular disease. Cardiovasc Pathol. 2002; 11:332–338. [PubMed: 12459434]

128. Yaman O, Yilmaz E, Bozlu M, Anafarta K. Alterations of intracorporeal structures in patients with erectile dysfunction. Urol Int. 2003; 71:87–90. [PubMed: 12845268]

129. Yokota H, Goldring MB, Sun HB. CITED2-mediated regulation of MMP-1 and MMP-13 in human chondrocytes under flow shear. J Biol Chem. 2003; 278:47275–47280. [PubMed: 12960175]

130. Zeeberg BR, Feng W, Wang G, Wang MD, Fojo AT, Sunshine M, Narasimhan S, Kane DW, Reinhold WC, Lababidi S, Bussey KJ, Riss J, Barrett JC, Weinstein JN. GoMiner: a resource for biological interpretation of genomic and proteomic data. Genome Biol. 2003; 4:R28. [PubMed: 12702209]

131. Zimmermann R, Panzenbock U, Wintersperger A, Levak-Frank S, Graier W, Glatter O, Fritz G, Kostner GM, Zechner R. Lipoprotein lipase mediates the uptake of glycated LDL in fibroblasts, endothelial cells, and macrophages. Diabetes. 2001; 50:1643–1653. [PubMed: 11423487]

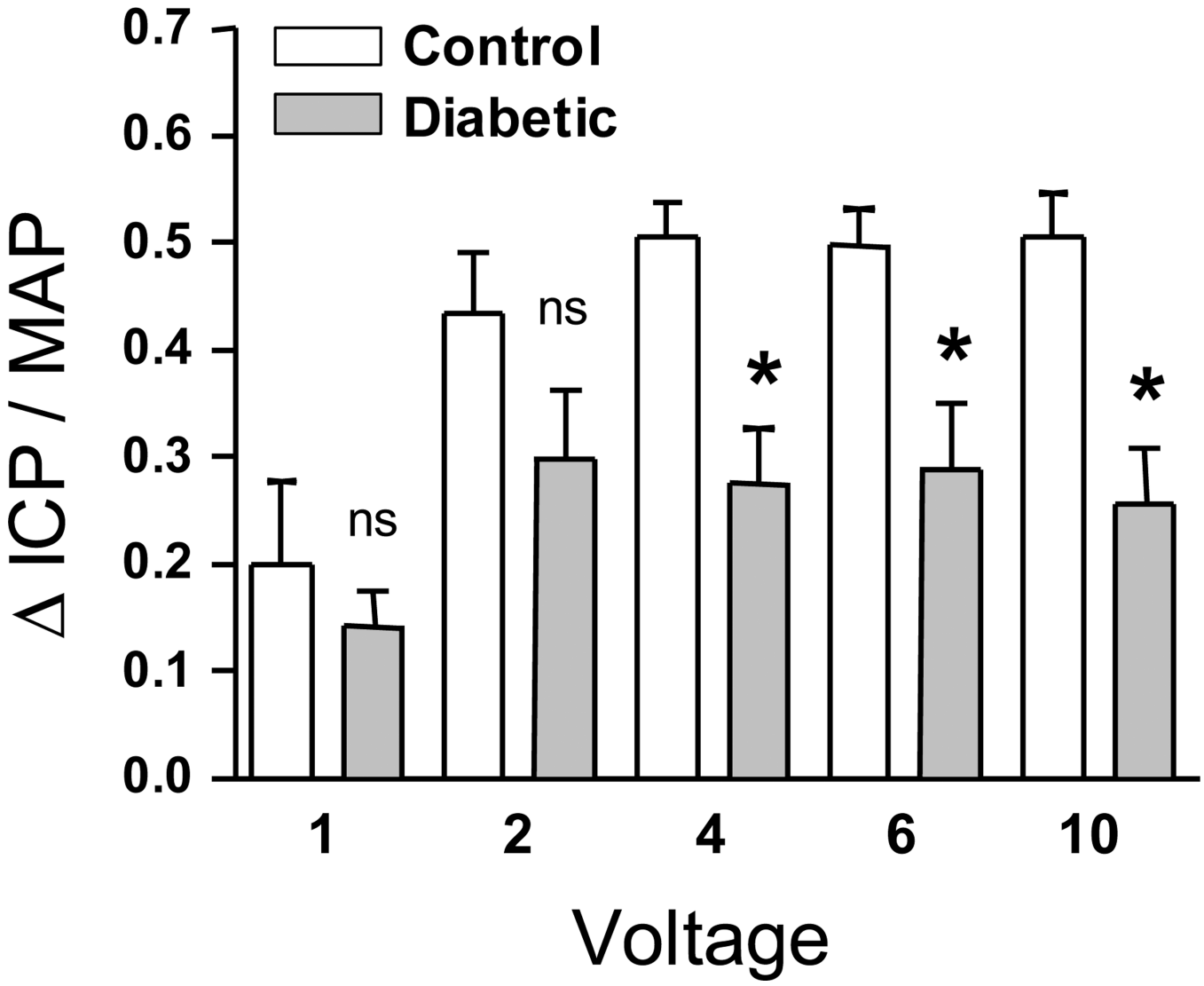

Figure 1.
Decreased erectile function in diabetic animals in response to cavernous nerve stimulation. The mean ΔICP/MAP (area under the curve for the ICP and MAP tracings during the 60s stimulation, mmHg·s) was lower at all voltages in diabetic rats (n=6) compared to control (n=8). Values are statistically significant at 4, 6, and 10V, *$p < 0.01$.

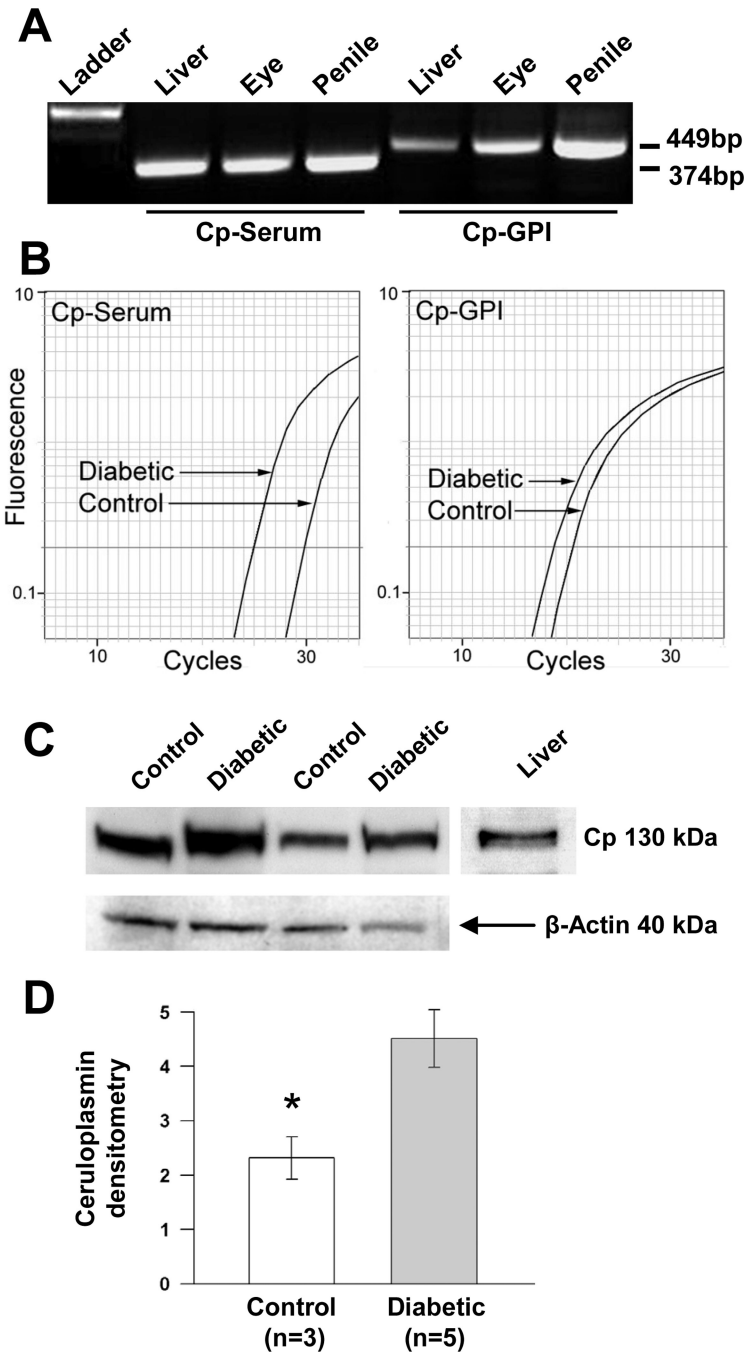

Figure 2.

Upregulation of ceruloplasmin splice variants in diabetic cavernosal tissue. A: conventional, non-quantitative PCR to confirm the expression of the known Cp mRNA splice variants in the penis using previously published primer sets, Cp-GPI (membrane anchored) and Cp-Serum (secreted) yield 449 and 374 base-pair products, respectively. Ladder indicates the lane of DNA markers with the 600 bp marker brightly displayed. B: representative amplification plots of real-time PCR comparing diabetic and control expression of Cp variants in cavernosal tissue. Average fold-upregulation in diabetic animals versus control (n=3) was 2.4 for Cp-GPI and 16 for Cp-Serum. C: representative Western blot of CP protein (~130kDa) content in the diabetic and control cavernosum, liver is shown as positive

control for CP. D: densitometric analysis of CP protein levels, expressed relative to β-actin for each corresponding sample, showed an approximately 1.9-fold increase in diabetic tissue versus control (* $p < 0.05$).

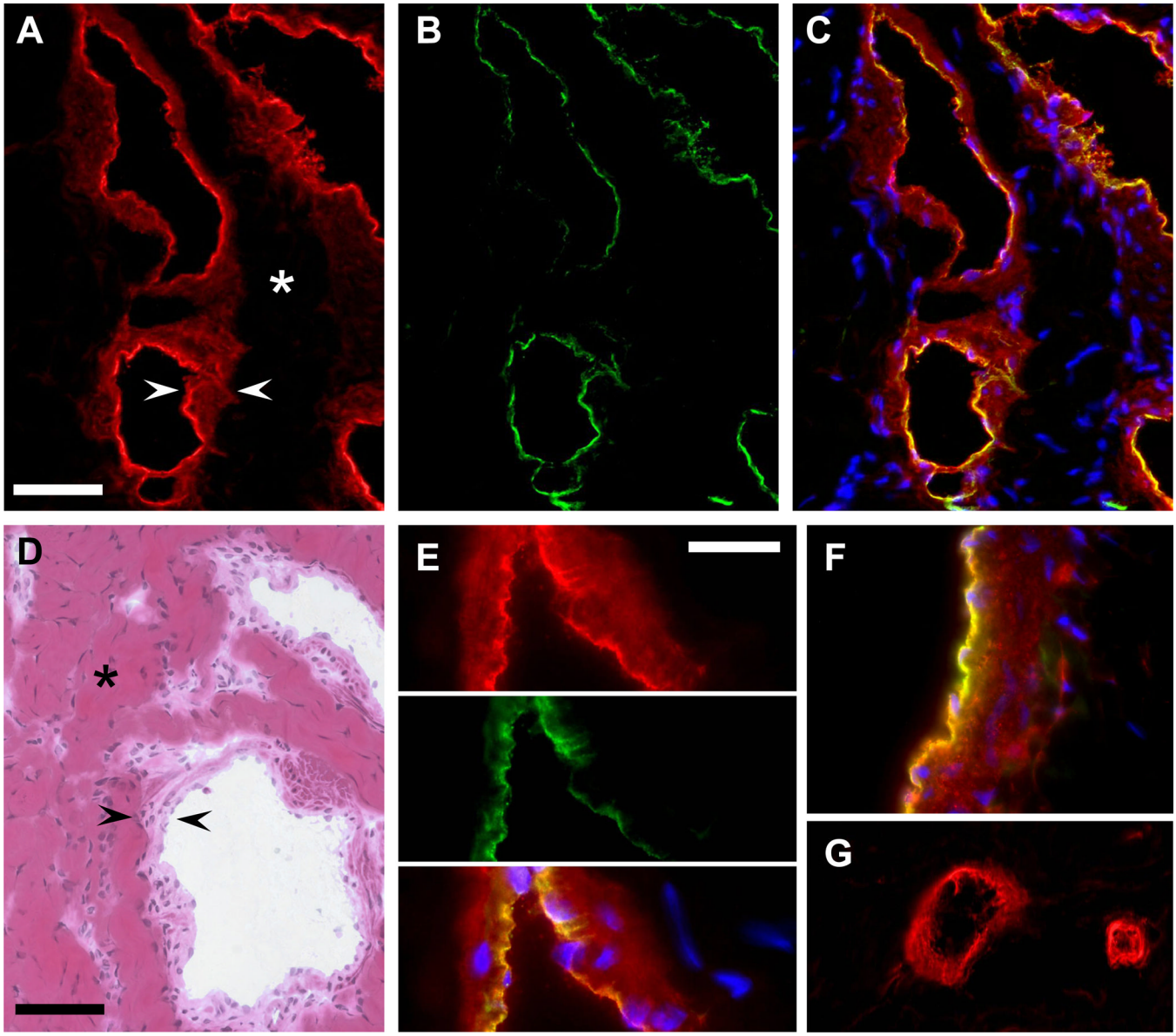

Figure 3.

Localization of ceruloplasmin protein to the sinusoids of the cavernosum. A: 40x, CP staining (red, Alexa 568) of cavernosal sinusoids (arrowheads). Asterisk marks the trabeculae which were largely unstained. B: The same tissue section was co-stained with CD31 (green, Alexa 488) to label the endothelium. C: merged CP (red), CD31 (green), and Nuclei (blue) stained images shows colocalization of CP and CD31 labeling in the endothelium (yellow). D: 40×, hematoxylin-eosin staining shows the general cavernosal architecture with collagen-based trabeculae (asterisk) lined by smooth muscle and endothelial cells (the SMC and EC layers are located between the black arrowheads). E: 100×, higher magnification of sinusoid labeled with CP (red) and CD31 (green). CP labeling of SMC layer with brightest staining colocalized with endothelial marker CD31 shown in the merged image as yellow. F: Penile dorsal vein co-stained with CP and CD31 antibody showing SMC and endothelial localization of CP. G: CP antibody labeling of microvessels adjacent to the cavernosum. A–D, scale bar = 50 μm. E–G, scale bar = 20 μm.

Physiol Genomics. Author manuscript; available in PMC 2014 January 27.

Table 1

A selection of the differentially expressed genes in the diabetic rat cavernosum with corresponding Affymetrix probe set ID, genes arranged based on functional categorization and similar Gene Ontology.

Affymetrix Probe ID	Gene Symbol	Gene Name	Fold Δ	*p*-value	Function
Elastin related					
1388142	(Cspg2)	chondroitin sulfate proteoglycan 2 (similar to)	−3.3	0.00002	proteoglycan binds Fbn1 in microfibrils
1388054	(Cspg2)	also known as versican	−2.6	0.00031	and involved in assembly of ECM and elastic fibers
1368171	Lox	lysyl oxidase	−3.0	5.7E-12	enzyme cross-links elastin and collagen
1368172	Lox	lysyl oxidase	−2.3	3.3E-08	and is expressed in remodeling or injured arteries
1371815	(Mfap2)	microfibrillar-associated protein 2 (similar to)	−2.6	0.00315	associated with elastin microfibrils
1387351	Fbn1	fibrillin 1	−2.1	0.00149	forms microfibrils associated with elastin
1367594	Bgn	biglycan	−1.9	0.00601	forms complex with elastin and Mfap2
1371369	(Col6a2)	collagen, type VI, alpha 2 (similar to)	−1.8	0.00391	associated with elastin microfibrils
1388111	Eln	elastin, also tropoelastin	−1.7	0.00159	tissue elasticity, substrate for Lox
Collagens					
1370864	Col1a1	collagen, type 1, alpha 1	−3.6	0.00003	fibril forming collagen, connective tissues
1388116	Col1a1	collagen, type 1, alpha 1	−2.5	0.00032	and provides tensile strength and stiffness
1387854	Col1a2	collagen, type I, alpha 2	−3.0	0.00003	fibril forming collagen, connective tissues
1370155	Col1a2	collagen, type I, alpha 2	−2.5	0.00058	
1370959	Col3a1	collagen, type III, alpha 1	−2.2	3.7E-07	component of reticular fibers in elastic tissues
1369955	Col5a1	collagen, type V, alpha 1	−3.0	0.00041	forms heterofibrils with type I and III collagens
1376099	Col5a1	collagen, type V, alpha 1	−2.3	0.00362	and forms interstitial matrix in various tissues
1370895	Col5a2	collagen, type V, alpha 2	−1.9	0.00001	similar functions as Col5a1
1373463	Col5a2	collagen, type V, alpha 2	−1.9	0.00017	
1368347	Col5a3	collagen, type V, alpha 3	−6.9	0.00144	similar functions as Col5a1
1384211	Col11a1	collagen, type XI, alpha 1	−3.9	5.3E-08	fibril forming collagen, articular cartilage
Other ECM related					
1367581	Spp1	secreted phosphoprotein 1 (osteopontin)	−11.8	0.01	multifunctional matricellular protein
1373911	(Postn)	periostin, osteoblast specific factor (similar to)	−3.4	0.00212	implicated in angiogenesis and SMC differentiation
1373401	(Tnc)	tenascin C (similar to)	−3.1	0.00545	multifunctional matricellular protein
1368657	Mmp3	matrix metalloproteinase 3 (stromelysin 1)	−3.0	0.00001	substrates include procollagenase, Sparc, Spp1

Affymetrix Probe ID	Gene Symbol	Gene Name	Fold Δ	*p*-value	Function
1389306	(Matn2)	matrilin 2 (similar to)	−2.9	1.3E-06	filament-forming protein widely distributed in ECM
1367562	Sparc	secreted acidic cysteine rich glycoprotein	−2.4	1.0E-07	matricellular protein, roles in adhesion
1367563	Sparc	also known as osteonectin	−2.0	1.6E-05	and fibrosis, angiogenesis, ECM remodeling
1368293	Cpz	carboxypeptidase Z	−2.1	0.00037	enzyme enriched in ECM, Wnt-binding
1370234	Fn1	fibronectin 1	−1.8	4.9E-06	glycoprotein, cell adhesion, migration, growth
1388932	Lama5	laminin, alpha 5	2.1	0.00058	proteoglycan component of basement membrane
1377428	Lama5	laminin, alpha 5	4.5	0.002	and component of laminin heterotrimeric complex
1371073	B4galt1	UDP-Gal:betaGlcNAc beta 1,4-galactosyltransferase, polypeptide 1	3.3	5.6E-10	selectin-ligand biosynthesis, cell adhesion
Response to Oxidative Stress					
1374070	Gpx2	glutathione peroxidase 2	4.0	0.00776	glutathione-dependent hydrogen peroxide reduction
1367995	Cat	catalase	2.2	1.9E-07	antioxidant enzyme, removes hydrogen peroxides
1367612	Mgst1	microsomal glutathione S-transferase 1	2.0	0.00041	protects against oxidative stress, lipid hydroperoxide
1370952	Gstm2	glutathione S-transferase, mu 2	1.8	0.0039	role in cellular resistance against oxidative stress
1387599	Nqo1	NAD(P)H dehydrogenase, quinone 1	1.7	0.01	protects against redox cycling and oxidative stress

(Gene Symbol) = identified as putative homolog to mouse and human genes, Homologene-NCBI. Fold change (Δ) is relative to control expression. Fold Δ and *p* value were estimated using Rosetta Resolver software based on 5 biological replicates for each diabetic and control groups. ECM = extracellular matrix. SMC = smooth muscle cell.

Table 2

Real-time PCR confirmation of array results for select genes.

Accession Number	Gene Symbol	Fold Δ		Description and/or functions	References
		PCR	Array		
NM_012532	Cp	4.3	3.3*	Ceruloplasmin; plasma metalloprotein made in liver that that binds copper, increased expression in diabetes, expressed in smooth muscle cells, inhibits eNOS, impairs vessel relaxation	9, 17, 19, 42
NM_139082	Bambi	4.2	4.7	BMP and activin membrane-bound inhibitor, homolog (Xenopus laevis); inhibits TGFβ signaling	87, 117
XM_214551	(Cidea)	3.5	2.6	Similar to cell death-inducing DFFA-like effector A; induces apoptosis	54
NM_053394	Klf5	2.7	3.3	Kruppel-like factor 5; transcription factor modulates SMC phenotype	51, 122
NM_012598	Lpl	2.7	2.6	Multifunctional enzyme, widely expressed including vascular smooth muscle cells, Lpl protein is detected on endothelium (no mRNA), overexpression impairs blood vessel relaxation	16, 27, 57
XM_238119	(Sema4b)	2.6	6.2	Similar to semaphorin 4B; class 4 semaphorins have transmembrane domain	35
NM_012520	Cat	2.4	2.2	Catalase; antioxidant with expression in response to oxidative stress	78
NM_053698	Cited2	2.4	2.5	Cbp/p300-interacting transactivator, with Glu/Asp-rich terminal domain, 2; transcriptional cofactor, represses HIF1α activity, negative regulator of MMP1 and 13	36, 116, 129
NM_007643	Cd36	2.3	2.2	Class B scavenger receptor, possible role in development of eNOS-related vascular dysfunction, absence may help protect against atherosclerosis	33, 64
NM_031535	Bcl2l1	2.1	2.3	Bcl2-like 1, BCL-2 protein family; anti-apoptotic signaling	120
NM_134455	Cx3cl1	1.8	3.6	Chemokine (C-X3-C motif) ligand 1 (also termed Fractalkine); upregulation in diabetic nephropathy, aortic SMC expression	18, 63
NM_017107	Ogt	1.8	1.5	O-linked N-acetylglucosamine (GlcNAc) transferase; GlcNAc onto proteins	2
NM_053402	Wnt4	1.8	2.2	Glycoprotein involved in genitourinary development, increased in renal fibrosis and wound healing, experimental overexpression disrupts normal vascular pattern formation in the testis	56, 69, 111
NM_053578	Atp6k	1.0	1.0	Vacuolar proton-ATPase subunit M9.2; vacuolar proton pump. No change detected.	
NM_012553	Ela2	1.0	4.5	Elastase 2; enzyme expressed in rat arterial beds, generates angiotensin II	104
NM_031825	Fbn1	−1.4	−2.1	Involved with microfibril assembly, is found in elastic connective tissues	62
J04035	Eln	−1.6	−1.7	Elastin, also tropoelastin; elasticity of tissues, substrate for Lox	62
AY007691	(Cspg2)	−1.9	−3.0*	Proteoglycan in vascular wall, expressed by SMC, upregulated in vascular injury	79, 83
NM_012656	Sparc	−2.0	−2.2*	Absence associated with changes in ECM assembly/composition and is reduced in vessels with Monckeberg's sclerosis (medial calcification)	12, 106
NM_012881	Spp1	−2.2	−11.8	Multiple reported roles in vascular calcification, remodeling, and vessel structure	81, 121
NM_173125	(Pdlim7)	−2.6	−3.1	PDZ and LIM domain 7 (also termed Enigma); LIM domains bind to protein kinases, whereas PDZ domain binds to actin filaments, upregulated by estrogen in cultured vascular SMCs	48, 123
NM_017061	Lox	−2.6	−2.7*	Cross-links elastin and collagen, secreted by smooth muscle, vessel remodeling	85, 109
NM_012618	S100a4	−3.1	−1.9	S100 calcium-binding protein A4; expression detected in aorta and SMC	24

Accession Number	Gene Symbol	Fold Δ PCR	Fold Δ Array	Description and/or functions	References
NM_019282	Cktsf1b1	−7.9	−5.8	Cysteine knot superfamily 1, BMP antagonist 1 (also termed Gremlin 1); induced in diabetic nephropathy, BMP antagonist actions increase FGF and sonic hedgehog expression	61, 70

Real-time PCR validation of various genes estimated to be differentially expressed based on the Resolver array analysis (p-value ≤ 0.01). Atp6k was selected as a gene whose expression was unchanged between groups based on array results. For PCR, relative changes in gene expression (fold Δ) were calculated using the $2^{-\Delta\Delta CT}$ method. Also, PCR fold Δ is relative to control cDNA while using Actb (Beta actin) expression as a reference gene. Array fold Δ in certain cases (*) is an average since the gene had multiple probe sets called significant. (Gene Symbol) = *Rattus norvegicus* transcript listed as "similar to" mouse and human gene, Homologene-NCBI. SMC = smooth muscle cell.